

Research Article

Cite this article: Martin SL, Sears E, James T, Sharpe S, Tidemann BD (2025). Structured, inbred, and plastic: the genome and population genetics of the weed false cleavers (*Galium spurium*). *Weed Sci.* **73**(e10), 1–21. doi: [10.1017/wsc.2024.79](https://doi.org/10.1017/wsc.2024.79)

Received: 3 June 2024

Revised: 6 September 2024

Accepted: 8 October 2024

Associate Editor:

Caio Brunharo, Penn State University




Keywords:

Auxin resistance; ddRAD tags; Rubiaceae, weed genome

Corresponding author:

Sara L. Martin; Email: sara.martin@agr.gc.ca

Structured, inbred, and plastic: the genome and population genetics of the weed false cleavers (*Galium spurium*)

Sara L. Martin¹ , Elizabeth Sears², Tracey James², Shaun Sharpe³  and Breanne D. Tidemann⁴ 

¹Research Scientist, Ottawa Research and Development Centre, Agriculture and Agri-Food Canada, Ottawa, Canada;

²Research Technician, Ottawa Research and Development Centre, Agriculture and Agri-Food Canada, Ottawa, Canada;

³Research Scientist, Saskatoon Research and Development Centre, Agriculture and Agri-Food Canada, Saskatoon, Canada and

⁴Research Scientist, Lacombe Research and Development Centre, Agriculture and Agri-Food Canada, Lacombe, Canada

Abstract

False cleavers (*Galium spurium* L.) is an aggressive weed from the Rubiaceae. Here we assemble a chromosome-scale draft of its genome, laying the foundations for determining the genetic basis of auxinic herbicide resistance and for systematic research into its polyphyletic genus. We use the genome to examine the population genetics of material from the Canadian Prairies and, in concert with a common greenhouse experiment, to examine whether the phenotypic variation observed in the field results primarily from genetic or environmental factors. The genome assembly covers approximately 85% of *G. spurium*'s expected 360-Mbp genome size, with 94% of BUSCO (Benchmarking Universal Single-Copy Orthologs) genes complete and most single copy (89%). Approximately 37% of the genome is repetitive elements and 35,540 genes were annotated using RNA-seq data, including 100 homologues for genes involved in, or potentially involved in, herbicide resistance. The genome shows strong synteny with other members of the Rubiaceae, including smooth bedstraw (*Cruciata laevipes* Opiz) and robusta coffee [*Coffea canephora* (Pierre ex Froehner)]. Double-digested RAD-seq data for the 19 populations from the Canadian Prairies indicated that *G. spurium* has high levels of population structure ($F_{ST} = 0.54$) and inbreeding ($F_{IS} = 0.86$) with low levels of heterozygosity ($H_O = 0.02$) and nucleotide diversity ($\pi = 0.0003$). Variation in flowering time and seed weight largely overlapped among populations grown in the greenhouse. A redundancy analysis investigating genotype–phenotype associations showed few associations between single-nucleotide polymorphism (SNP) variation and these characteristics. In contrast, the majority of SNPs under selection were associated with mericarp hook density. This suggests that for most traits, environmental variation rather than genetic variation likely underlies phenotypic differences observed in the field. Several genes of interest, including several homologues involved in the assembly of the Skp1-Cullin-F-Box IR1/AFB E3 ubiquitin ligase complex (e.g., *CAND1*, *ECR1*), are located in areas of the genome with evidence of selection and are targets for further investigation.

Introduction

Rubiaceae is the fourth-largest plant family and contains several economically important crop plants, including one essential for scientific research—coffee (*Coffea arabica* L.). *Galium* is the largest and most widespread genus within the tribe Rubieae with 600 to 700 species and a cosmopolitan distribution that primarily centers on temperate regions (Chen and Ehrendorfer 2001; Soza and Olmstead 2010). Although *Galium* species have been used as a coffee substitute (Turner and Szczawinski 1978), the main economic impact of the genus is as weeds, with 18 listed as weeds in jurisdictions around the world (Holm et al. 1991).

A particularly problematic species is false cleavers (*Galium spurium* L.) ($2n = 20$, $2C = 0.72$ pg, 360 Mb), which can cause significant crop losses in cereals, canola (*Brassica napus* L.), and sugar beet (*Beta vulgaris* L.) (Malik and Vanden Born 1988). The large variability of *G. spurium* has resulted in many synonyms and misidentifications with other taxa of *Galium*, and adding to the confusion and likely to morphological diversity, the species is considered to be a parental lineage within the polymorphic polyploid complex with *Galium aparine* L. (Chen and Ehrendorfer 2001). This occasionally results in *G. spurium* not being recognized in keys for the genus, which exacerbates difficulties in distinguishing the species by limiting the number of locally relevant keys providing for this separation (Gleason and Cronquist 1991; Looman and Best 1979; Voss and Reznicek 2012). Differentiation of *Galium* species based on incompletely represented morphology can be extremely difficult. However, *G. aparine* is found in temperate

© Crown Copyright - His Majesty the King in Right of Canada, as represented by the Minister of Agriculture and Agri-Food Canada, 2024. Published by Cambridge University Press on behalf of Weed Science Society of America. This is an Open Access article, distributed under the terms of the Creative Commons Attribution licence (<https://creativecommons.org/licenses/by/4.0/>), which permits unrestricted re-use, distribution and reproduction, provided the original article is properly cited.



zones around the world and at higher elevations in the tropics, often in non-agricultural settings such as moist deciduous woods. *Galium spurium* has a similarly broad distribution, but typically occurs in sunnier, more open, and disturbed environments such as fencerows, roadsides, and waste grounds. It is considered to be the weedier and more aggressive of the two species (Malik and Vanden Born 1988). As the species climbs and then grows over top of crop species, it can cause lodging and difficulties with harvest while reducing yield. A similar seed size and shape also make it a serious contaminant of canola (Hall et al. 1998). The abundance of the species has rapidly increased across the Canadian Prairies since the 1970s, and it is now one of the top 10 most abundant weeds (Leeson et al. 2005).

The evolution of herbicide resistance has added complications to the control of *G. spurium*, with resistance to acetolactate synthesis inhibitors (ALS) and synthetic auxins such as quinclorac reported (Beckie et al. 2012; Hall et al. 1998; Heap 2023). The genetic basis of ALS-inhibitor resistance is a point mutation at the target site. However, while the genetic basis of quinclorac resistance has been shown to be controlled by a locus distinct from the ALS point mutation and to be a single, recessive nuclear trait in material from Alberta, the locus involved has not yet been identified (Van Eerd 2004; Van Eerd et al. 2004). The spread of ALS-inhibitor resistance has been documented in the Canadian Prairie herbicide resistance surveys since 2007 (Beckie et al. 2013), but the spread and extent of the auxin-resistant biotype is currently unknown.

Here we assemble a chromosome-level draft for the genome of *G. spurium* and situate it in its evolutionary context by comparing its genomic structure to that of its nearest relatives with available chromosome-level genome assemblies: crosswort (*Crucifera laevipes* Opiz), field madder (*Sherardia arvensis* L.), leptodermis (*Leptodermis oblonga* Bunge), and robusta coffee (*Coffea canephora* Pierre ex Froehner). We then use the genome to facilitate investigation of the species' population biology. Specifically, we examine the diversity and structure of 19 populations collected from Alberta and Saskatchewan, Canada, using reduced genome representation (ddRAD tags) (Peterson et al. 2012). We complement this genetic analysis with data from a common garden experiment conducted in the greenhouse to examine whether phenotypic variation observed in the field is the result of genetic or environmental variation. Finally, we examine homologues of genes known or suspected to be involved in the evolution of herbicide resistance and examine their proximity to single-nucleotide polymorphisms (SNPs) showing evidence of selection. This work provides insights into the population genetics and genomics of this tenacious weed species while providing a foundation for future work examining the genetic basis of herbicide resistance and, more broadly, the systematics of this complicated, currently polyphyletic, genus (Yang et al. 2018).

Materials and Methods

Plant Material and Phenotypic Measurements

Seed was collected in bulk from 19 locations in Canada, 11 in Alberta and 8 in Saskatchewan (Figure 1), and sent to the Ottawa Research and Development Centre in Ottawa, ON, Canada for growth and analysis. While initial plans were to use a random "W" sample across fields selected for collection, drought conditions in the year of collection severely limited the availability of *G. spurium* populations. As a result, the *G. spurium* populations were collected

in bulk with no set protocol, aside from collecting enough seed from the population at each location to allow conductance of various planned experiments with the material. A voucher for the individual sequenced to chromosome-level is available in the DAO herbarium with the bar code: 01-01667380. The map of locations was produced in R (v. 4.1.1 "Kick Things") (R Core Team 2021) using the packages: MAPS (Brownrigg et al. 2022), RNATURALEARTH (South 2017), SF (Pebesma 2018), TIDYVERSE (Wickham et al. 2019), and UNITS (Pebesma et al. 2016).

Seeds were sown into Pro-Mix® soil (soil, peat, and sand; 1:2:1; Pro-Mix, Rivière-du-Loup, QC, Canada) in 10-cm-diameter pots and placed in the greenhouse with day and night temperatures set to 20 C days and 18 C nights and a 16-h light cycle. In the first experiment, germination rates were tested, with 20 seeds per population placed on potting soil, covered lightly, and then scored for emergence weekly for 1 mo. In the second experiment, a common garden experiment, 19 to 22 plants per population were grown and randomly assigned a location in the greenhouse and were re-randomized 2 wk after planting, but were too large at 4 wk for an additional round of randomization. These plants were grown in a common environment to evaluate their morphological and phenotypic characteristics while minimizing the effect of environmental variation. Plant height was measured using a measuring tape each week for 3 wk starting when the first plants began flowering until the majority of the plants were too large and had to be folded over and tied to stakes. Plant height was measured from the soil surface to the most distal end of the longest branch. Flowering status was evaluated in three categories—vegetative, flowering but no seeds, and seeds forming—and was recorded weekly for the 3 wk over the same period. Flower and seed size was measured using a dissecting scope and digital calipers for three flowers or seeds of each of three individuals from each population. Plants were harvested after flowering by clipping the stems at the soil surface and placing them in a large paper bag. These bags were then placed in a drying oven at 30 C for 7 d before weighing until seed cleaning to keep the material dry. Total plant (Ohaus Voyager Pro Precision, Parsippany, NJ, USA) and total seed weight (Mettler-Toledo AT200, Columbus, OH, USA) as well as three replicates of 100-seed weight were measured. The total seed weight and average 100-seed weight were used to estimate seed production, unless fewer than 300 seeds were produced. In these cases, the seeds were counted exactly. Seed trichome density was scored using a dissecting scope as naked, sparsely hooked, or densely hooked (Figure 2).

Flow cytometry was conducted to verify the DNA content of each individual included in the greenhouse experiment analysis according to the procedure followed in the Martin Laboratory (Martin et al. 2017), except that individuals were quickly screened with a single run. Radish (*Raphanus sativus* L.) was used as the internal standard. The FLOWPLOIDY package (Smith et al. 2018) in R was used to analyze data from the flow cytometer.

Statistical Analyses of Phenotypic Data

The statistical analysis of phenotypic data was conducted with R. Specifically, phenotypic data were evaluated following Box-Cox transformation from the MASS package (Venables and Ripley 2002) using one-way analyses with the function *oneway.test*, which uses Welch tests that do not assume equal variances across populations as the fixed variable followed by Tukey's post hoc test. The proportions of plants germinating, flowering, or with seed at different time points were analyzed with Pearson's chi-square test

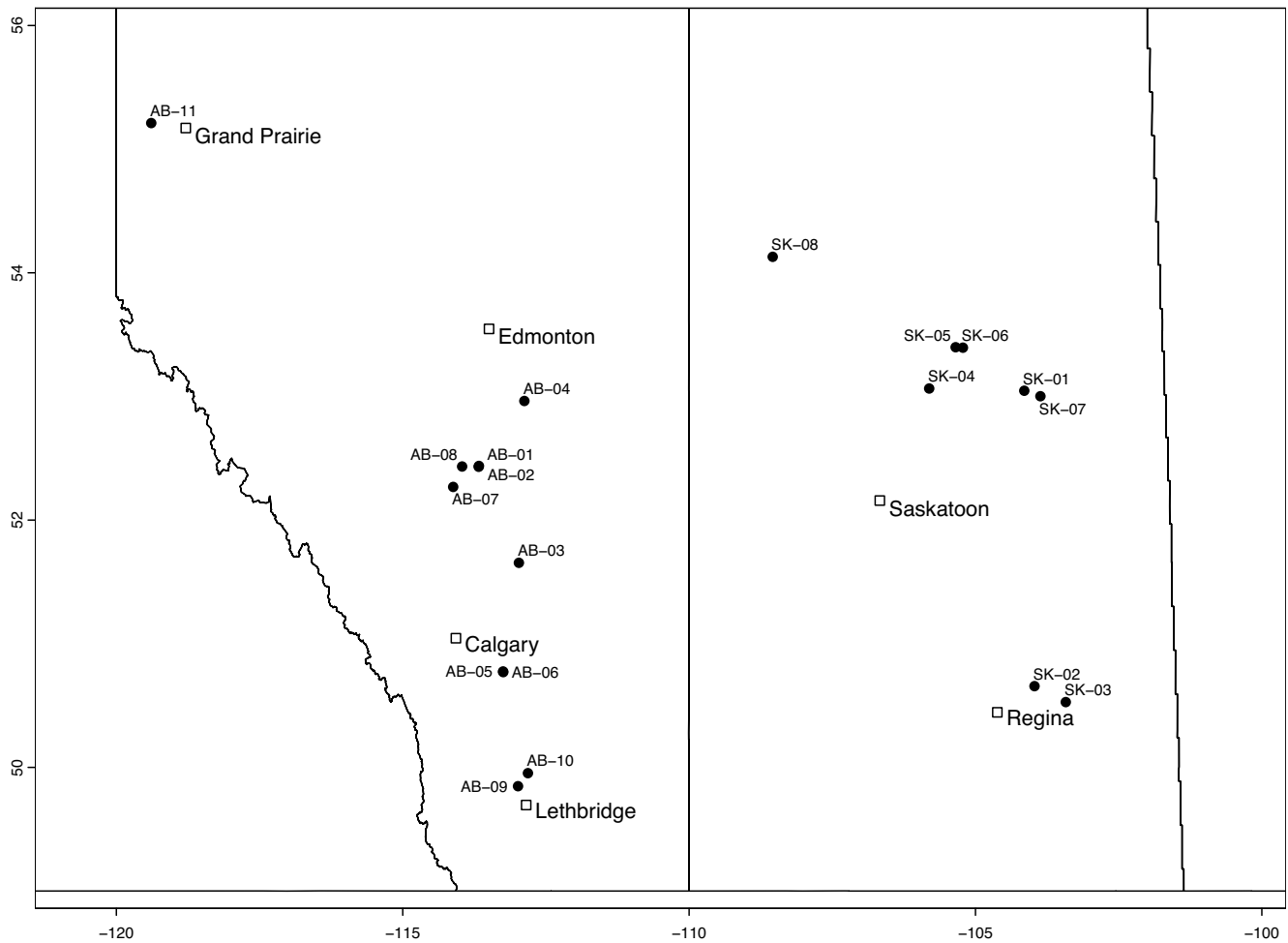


Figure 1. Map of the Canadian Prairie provinces of Alberta and Saskatchewan indicating locations for sample populations collected for use in this research, with latitude indicated on the left and longitude indicated along the bottom.

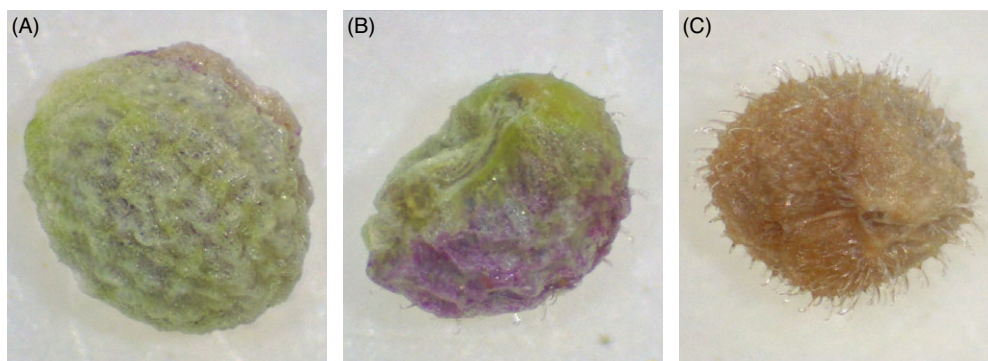


Figure 2. The three visual categories scored for hook density on the mericarps of *Galium spurium*: (A) naked, (B) sparsely hooked, and (C) densely hooked.

for binary variables (*chisq.bintest*) with a Benjamini and Hochberg correction for the P-values to control family-wise error rates from the package RVAIDEMEMOIRE (Hervé 2022). Exploration of the data and analyses was aided by functions in the CAR package (Fox and Weisberg 2019). Confidence intervals for proportions were estimated using the score method (Newcombe 1998). The function *mulcompLetters* from the MULTCOMPVIEW package (Graves et al. 2019) was used to simplify the results of post hoc pairwise comparisons for plotting. Additionally, functions from HMISC

(Harrell 2022) and PLOTRIX (Lemon 2006) were used for visualization.

DNA and RNA Sampling and Sequencing

One individual was chosen for genome assembly, and leaf tissue was collected on dry ice before extraction using the protocol published by Workman et al. (2018). High-molecular-weight DNA was extracted, using a Nanobind Plant Nuclei Big DNA kit

(Circulomics, Baltimore, MD, USA), followed by a Short Read Eliminator Kit (Circulomics), following the manufacturer's directions. DNA was first quantified with an Invitrogen™ Qubit™ (Thermo Scientific, Waltham, MA, USA) using the dsDNA HS (high-sensitivity) assay according to the manufacturer's instructions. Following quantification, DNA was then assessed for quality (impurities and fragment size) using a DropSense (Trinean, Pleasanton, CA, USA) and the Agilent TapeStation 4200 (Agilent, Santa Clara, CA, USA) on the Genomic DNA Screentape. Sequencing was completed using 4 Flow Cells on the Oxford Nanopore Technology MinION system (ONT; Oxford Nanopore Technologies, Oxford Science Park, UK). DNA was also sent to Genome Quebec for sequencing of Illumina 150-bp paired-end reads.

To facilitate annotation of the genome, RNA was extracted from rosette leaves. Tissue was first flash frozen in liquid nitrogen and stored at -80°C until ready for extraction. RNA extraction was performed on 50 mg of rosette tissue using the Qiagen RNeasy Plant Mini Kit (Qiagen, Germantown, MD, USA) according to the manufacturer's instructions, adding an extra wash step to ensure a thorough flushing of the column. RNA was first quantified using a NanoDrop™ One (Thermo Scientific), then assessed for quality using a DropSense (Trinean) and the Agilent TapeStation 4200 (Agilent) on the RNA Screentape following the manufacturer's instructions. Once it was confirmed that RNA samples met the required parameters for sequencing, three samples were sent to BGI (BGI, San Jose, CA, USA) for mRNA library preparation and sequencing of 24 million 150-bp paired-ends per sample.

DNA was extracted using the NucleoSpin-96 Plant II kit (Macherey-Nagel, Dueren, Germany) (supplied by D-Mark Biosciences) for all individuals grown in the greenhouse experiment and sent to the University of Laval for ddRAD-tag library creation and to Genome Quebec for sequencing (Peterson et al. 2012).

Packages in R were then used to analyze or visualize the data, including functions from APE (Paradis and Schliep 2019), APEX (Schliep et al. 2020), BIOSTRINGS (Pagès et al. 2021), GEOSPHERE (Hijmans 2022), GGPLOT2 (Wickham 2016), GRAPH4LG (Savary et al. 2020), IRANGES (Lawrence et al. 2013), MSA (Bodenhofer et al. 2015), PHANGORN (Schliep 2011), PLYR (Wickham et al. 2022), RSAMTOOLS (Morgan et al. 2021), SEQINR (Charif and Lobry 2007), and STRINGR (Wickham 2022).

Genome Assembly and Annotation

Long-read ONT data (116X coverage) were called with Guppy (v. 5.0) and assembled using CANU (v. 2.2) (Koren et al. 2017). Contigs that represented the chloroplast were removed based on identity scores and length from Mummer (v. 4.0) (Marçais et al. 2018). The remaining contigs were checked using Blobtools (v. 1.1.1) to determine whether they represented contaminants (Laetsch and Blaxter 2017). However, no appreciable contamination was detected. This assembly was then polished three times using the Illumina data (113X coverage) using Pilon (v. 1.23) (Walker et al. 2014) after alignment with Burrows-Wheeler Alignment tool (BWA) (0.7.17) (Li and Durbin 2009). The polished assembly was scaffolded into a chromosome-level assembly by Phase Genomics (Seattle, WA, USA) using their proprietary pipeline and chromosomal conformation data (HiC) after processing of DNA with a Proximo Hi-C 2.0 Kit in the Martin Laboratory. Mummer and the Whole-Genome

Duplication Integrated analysis tool kit (WGDI v. 0.6.1) (Sun et al. 2022) were used to compare *G. spurium*'s genome with those of *C. laevipes* (GCA_963678965.1), *S. arvensis* (GCA_948330725.1), *L. oblonga* (Guo et al. 2021), *C. canephora* (AUK_PRJEB4211_v1), and common milkweed (*Asclepias syriaca* L.) (GCA_027405835.1). The genome assembly of *G. spurium* was assessed using QUASt v. 5.1.0rc1 (Gurevich et al. 2013), BUSCO (5.4.2, with the embryophyte_odb10 dataset of 2,192 genes) (Simao et al. 2015), and Samtools v. 1.9 (Li et al. 2009). MCScanx (Wang et al. 2012) was used to produce files for analysis with WGDI. The genome assembly is available as National Center for Biotechnology Information (NCBI) BioProject PRJNA1143567, on the International Weed Genomics Consortium online database WeedPedia (<https://www.weedgenomics.org/species/galium-spurium>), and from the corresponding author on reasonable request.

RNA sequence data were trimmed, cleaned, and filtered using SOAPnuke (v. 2.1.5) (Chen et al. 2018) and aligned to the genome using HISAT2 (v. 2.2.1) (Kim et al. 2019). Ninety-nine percent of the 72 million read pairs mapped to the genome. RepeatModeler (v. 2.0.3) (Smit and Hubley 2008–2015) and RepeatMasker (v. 4.1.2.p1) (Smit et al. 2010–2013) were used to generate a masked version of the genome. The BRAKER pipeline (v. 1.9) (Brůna et al. 2021; Hoff et al. 2019) was used to produce annotations based on this masked genome and the hints files generated by HISAT2. This pipeline relied on AUGUSTUS (Stanke et al. 2008), GeneMark-ET (Lomsadze et al. 2014), and Samtools. This procedure was also followed to add annotations to the genome of *L. oblonga* using RNA-seq data downloaded from the NCBI's Sequence Read Archive (SRR9839476) to allow comparative analysis with *G. spurium* using WGDI and GENESPACE (Lovell 2023; Lovell et al. 2022). GENESPACE uses other tools, including OrthoFinder (Emms and Kelly 2018, 2019), which constructed the phylogeny of the species included here using the STAG method. Following masking, AUGUSTUS was used to annotate the genomes of *C. laevipes*, *S. arvensis*, and *A. syriaca*, with tomato (*Solanum lycopersicum* L.) as the model.

Repetitive DNA was annotated using the Extensive de novo TE Annotator (EDTA v. 1.8.3) (Ou et al. 2019), which relies on LTRHarvest (Ellinghaus et al. 2008), LTR_Finder (Xu and Wang 2007), LTR_Retrieve (Ou and Jiang 2018), TIR-Learner (Su et al. 2019), Generic Repeat Finder (Shi and Liang 2019), HelitronScanner (Xiong et al. 2014), and TESorter (Zhang et al. 2019). LTRHarvest, LTR_Finder, and LTR_Retrieve were also used to calculate the LTR Assembly Index (LAI) (Ou et al. 2018). The genome sequence was also analyzed to detect Helitrons with EAHelitron (Hu et al. 2019).

Genes that could be involved in the evolution of herbicide resistance were identified through homology using blastp, the amino acid sequences of the genes identified using the BRAKER pipeline, and amino acid sequences of the genes of interest downloaded from GenBank or The Arabidopsis Information Resource (TAIR) (Supplementary Table 1). A cutoff of $1\text{-e}50$ was used to identify the best hits from these searches of the annotated proteins with score considered as a secondary indication to eliminate hits that had much smaller scores ($<50\%$) than the best hit for the reference protein. BLAST was run on the coding sequence for the protein (Supplementary Table 2) to cross-check that the best hits (Supplementary Table 3) with identifications indicated that the protein of interest had been likely been identified.

SNP Calling and Population Genetics Analyses

SNP calling was completed for the RAD-seq data using the reference-based pipeline in STACKS (v. 2.6) (Catchen et al. 2013) after alignment to the genome using BWA with the parameter (–L) for reducing soft clipping set to 500 (Li and Durbin 2009). Following the creation of the variant call file (vcf) by STACKS, data were further filtered using VCFtools (0.1.16) (Danecek et al. 2011) using the recommendations of O’Leary et al. (2018) to create two datasets for further analysis. STACKS initially identified 25K loci covering 6.7 million bp of the genome with 86K variants. The first filtered dataset included only genotypes with a read depth of greater than 5, loci with a mean read depth greater than 15, SNPs with a quality greater than 20, and SNPs with a minimum allele count greater than 3. These data contained just over 40K SNPs for 365 individuals with less than 1% missing and were used for examining genome-wide nucleotide diversity. This 40K set was further filtered for missingness following the O’Leary protocol (O’Leary et al. 2018) and thinned so that SNPs were at least 500 bp apart to reduce linkage. This second dataset contained just under 4K SNPs with less than 1% missing for 337 individuals and was used for examining population structure, the association between genetic and morphological variation, and evidence of selection. VCFtools was also used to calculate nucleotide diversity, with the remaining population summary statistics calculated with hierfstat (Goudet and Jombart 2022). A Mantel test (mantel.randtest::ade4) (Thioulouse et al. 2018) was used to determine whether there was a relationship between genetic and geographic distance, and redundancy analysis (vegan::rda) (Oksanen et al. 2022) was used to determine whether the morphological variation observed in the greenhouse was associated with variation within the SNPs. The R package PCADAPT (v. 4.3.5) was used to examine linkage disequilibrium and to look for evidence of SNPs in regions under selection with the final analysis using $K = 5$, linkage disequilibrium parameters set to $size = 200$ and $threshold = 0.1$, and a minimum minor allele frequency of 0.02 (Luu et al. 2017; Privé et al. 2020). This method examines association between population structure and genetic variants with the assumption that outlying variants are indicative of local adaptation (Privé et al. 2020). Tools for population genetics and genomics in R were used to analyze and visualize the SNP data, including functions from the following packages: ADEGENET (Jombart 2008), CIRCLIZE (Gu et al. 2014), COLORSPACE (Zeileis et al. 2020), DARTR (Mijangos et al. 2022), GVIZ (Hahne and Ivanek 2016), GWSCAR (Flanagan 2023), MAGRITTR (Bache and Wickham 2022), PEGAS (v. 1.1) (Paradis 2010), PHYTOOLS (v. 1.2-0) (Revell 2012), PNG (Urbanek 2022), POPPR (Kamvar et al. 2014), PINFSC50 (Knaus and Grünwald 2016), PSYCH (Revelle 2023), QVALUE (Storey et al. 2022), VARIANTANNOTATION (v. 1.42.1), and VCFR (Knaus and Grünwald 2016).

ChatGPT

In line with suggestions on how to improve time use efficiency in research (Pividori 2024) ChatGPT version 4 (OpenAI 2024) was used to reformat the references from EndNote Style “Weed Science J” after adding a DOI field for journal articles using the following prompt “I want you to pretend you are an editor at a scientific journal and reformat these references using these 9 criteria. 1. Journal names should not be in italics. 2. Author names should be in plain text. 3. DOIs should not be hyperlinks. 4. URLs should not be hyperlinks. 5. Plant scientific names should be in italics. 6. Plant names in English should not be in italics. 7. References should not

Table 1. Genome assembly statistics for *Galium spurium*.

Metric	Main assembly
Contigs ($\geq 50,000$ bp)	10
Total length	313,817,154
N50	31,727,068
NG50	30,373,747
Ns per 100 kbp ^a	3.9
BUSCO (eudicots_odb10)	
Complete (C)	2,192 (94%)
Complete single copy (S)	2,081 (89%)
Complete duplicated (D)	111 (5%)
Fragmented (F)	44 (2%)
Missing (M)	90 (4%)

^aNumber of base pairs represented with N rather than a sequenced nucleotide usually as a result of Ns placed between contigs during scaffolding.

be numbered. 8. Only proper names should be capitalized in the reference titles. 9. The journal names should be abbreviated based on the abbreviations listed at this website <https://woodward.library.ubc.ca/woodward/research-help/journal-abbreviations/>.” References were then checked and corrections made where necessary.

Results and Discussion

With the evolution of herbicide resistance, it is becoming increasingly important to be able to correctly identify weed species, comprehend their biology well enough to enable integrated management techniques, and understand the genetic basis of herbicide resistance so that individuals with these resistances can be identified. As a result, having the genetic tools to accomplish these goals is key. *Galium spurium* is a weedy species that grows up and over crops, causes lodging, reduces yield quantity and quality, and creates difficulties at harvest (Hall et al. 1998). It has developed herbicide resistance and belongs to a large genus of difficult to identify species. Here we produce a chromosome-level assembly of *G. spurium*, annotate it with RNA-seq data, and then use the genome in investigations of population genetics and to examine patterns of selection across the genome. This represents a foundational step toward identifying the genetic basis of auxinic herbicide resistance and clarifying evolutionary relationships within *Galium*.

Genome Assembly and Annotation

The flow cytometry estimates for 2C DNA content for *G. spurium* accessions grown in the greenhouse ranged from 0.71 to 0.74 pg with an average of 0.72 pg (SD ± 0.02) and indicated a haploid genome size of approximately 360 Mbp. The chromosome-level draft sequence produced for *Galium spurium* covers 85% this expected genome size and includes 94% of the expected core eukaryotic genes. The initial assembly of the *G. spurium*’s genome from the long-read ONT data (116X coverage) using CANU resulted in a draft assembly with 290 contigs with an NG50, the sequence length of the shortest contig at half the expected genome size when combined with the larger contigs, of 10.7 Mb and total assembly size of 318.5 Mb. A total of 128 of these contigs were placed on 10 scaffolds by Phase Genomics using Hi-C data, resulting in a chromosome-level assembly (Table 1). After the assembly was polished with Pilon, analysis with BUSCO indicated 94% of the expected genes were complete, with the vast majority

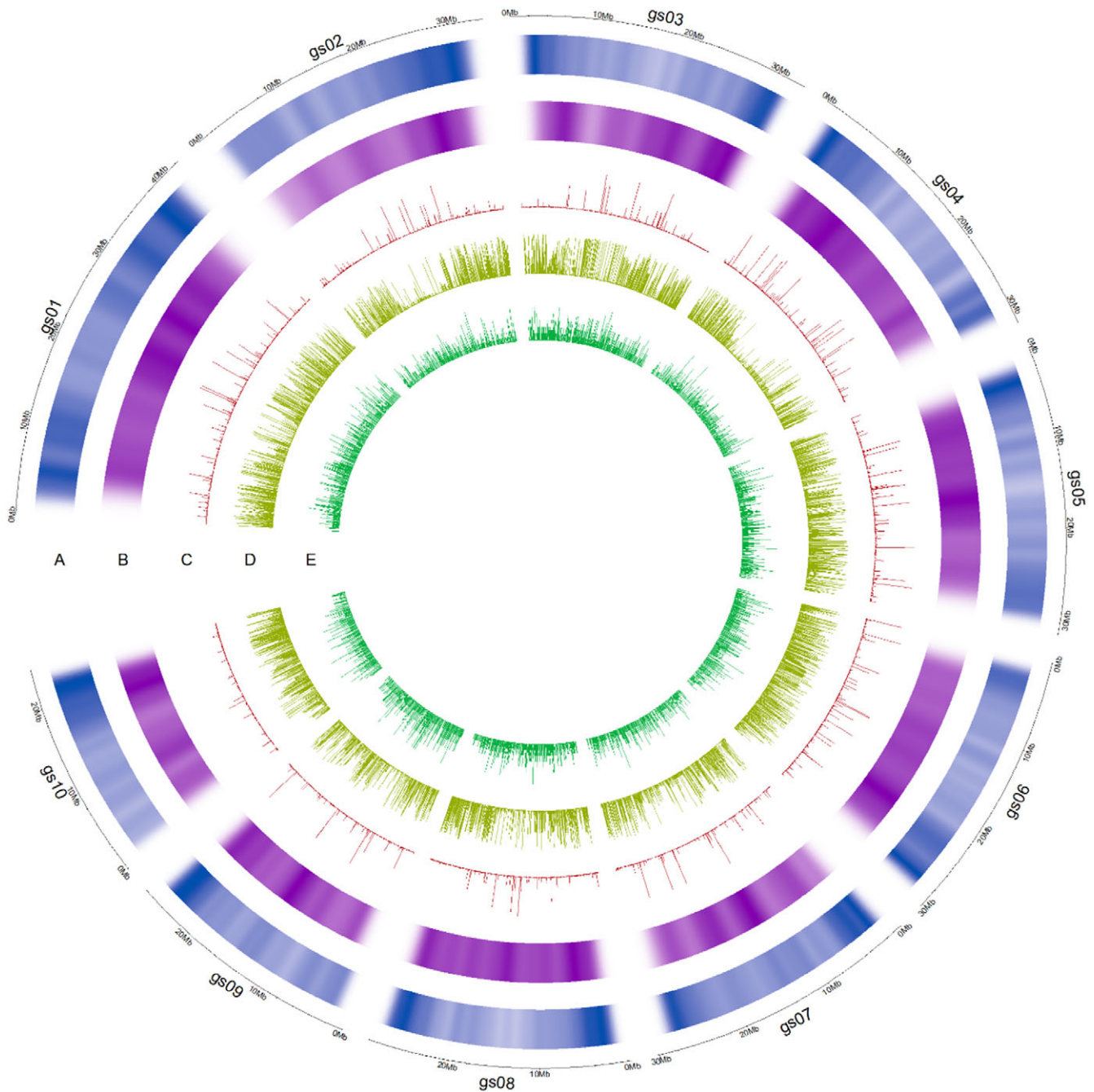


Figure 3. Circle plot of the *Galium spurium* genome with (A) gene density, (B) single-nucleotide polymorphism (SNP) density, (C) heterozygosity, (D) alternative allelic frequency, and (E) long terminal repeat frequency. An indication of chromosome length is plotted along the outside edge.

(89%) represented in a single copy and a minority (5%) found to be duplicated. Just under 150 million RNA data reads were used to annotate the genome, with 98% of these aligning to the genome. The BRAKER pipeline identified and annotated 35,549 genes based on this data, with 32,269 genes annotated using the same pipeline and downloaded data for *L. oblonga*. Repeat annotation using EDTA indicated that 37% of the genome was composed of repetitive elements, with the largest proportion of these identified as class 1 retrotransposons of the “Gypsy” type (11.5%) (Figure 3). Helitron density was assessed by EAHelitron as 6.7, and the LAI was 18.27, indicating that the genome meets the level of completeness for a reference-level genome (Ou et al. 2018).

Comparative Genomics

The genome of *G. spurium* has 10 chromosomes, but for the genus, other genera in the Rubiaceae, and in sister families such as the Apocynaceae, the more common base chromosome number is $n = 11$. Rubiaceae is divided into three subfamilies: Rubioideae, which includes *Galium*; Ixoroideae, which includes *Coffea*; and Cinchonoideae, which includes *Cinchona* (sources of quinine) (Bremer 2009; Stevens 2017). *Galium*, *Cruciata*, and *Sherardia* are all within the tribe Rubieae (Rubioideae), while *Leptodermis* is in a different tribe—the Paederieae (Rubioideae). As a result, *C. laevipes* ($n = 11$) and *S. arvensis* ($n = 11$) are the currently

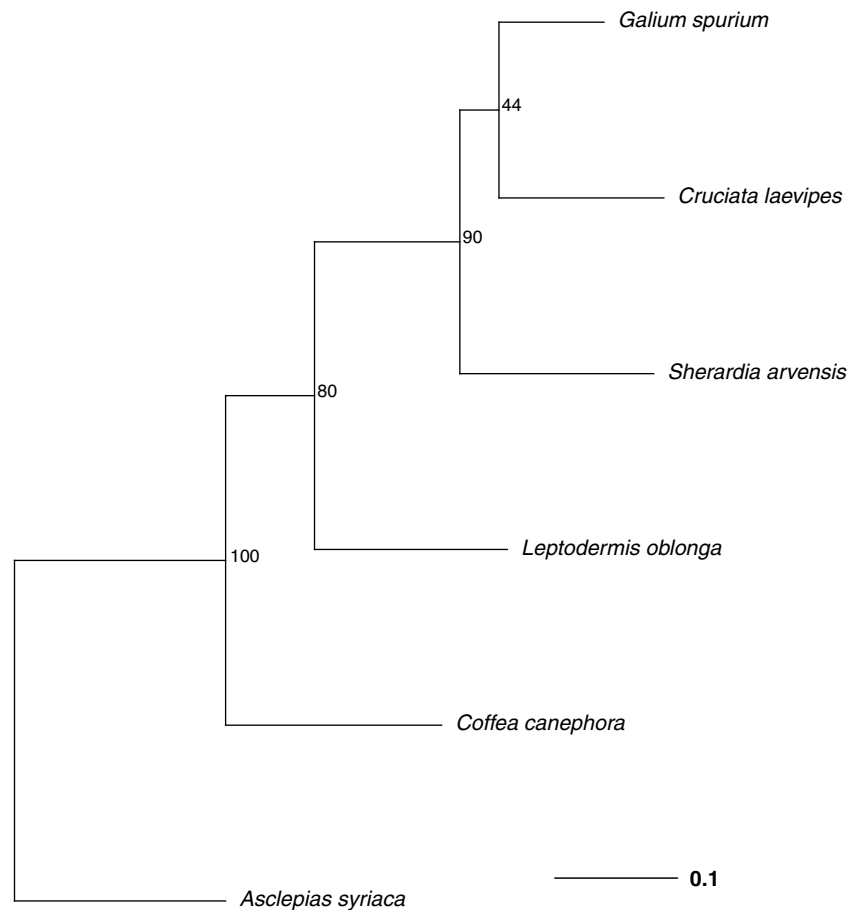


Figure 4. A phylogenetic tree indicating the evolutionary relationships among species studied here produced by OrthoFinder. The values at the nodes indicate support calculated by OrthoFinder using the Species Tree Inference from All Genes (STAG) method and indicates the proportion of orthogroup trees that had the bipartition. *Galium*, *Cruciatia*, and *Sherardia* are all within the tribe Rubieae (Rubiaceae), while *Leptodermis* is in the tribe Paederieae (Rubiaceae), and *Coffea canephora* is in a different subfamily, Ixoroideae. *Asclepias syriaca* is an outgroup from the Apocynaceae.

available chromosome-level assemblies that are most closely related to *G. spurium* with this chromosome number followed by *L. oblonga* ($n = 11$), and then more distantly by *C. canephora* ($n = 11$) and *A. syriaca* ($n = 11$), which is an out group from the Apocynaceae (Stevens 2017; Figure 4).

The genome of *G. spurium* shows strong synteny with the genomes of the other species from the Rubiaceae (Figures 5 and 6), including *C. canephora*, despite the divergence of their genera approximately 68 MYA (Kumar et al. 2022) (Figure 6B). Three chromosomes are largely syntenic when the genomes of *C. laevipes* and *G. spurium* are compared; *G. spurium*'s chromosomes 6, 7, and 10 show strong synteny with *C. laevipes*'s chromosomes 5, 7, and 9, respectively. However, there is no clearly identifiable mechanism, neither end-to-end joining nor nested chromosome fusion (Lysak 2022), that contributed to chromosome number reduction in *G. spurium* (Figure 6A). Rather, the genes from the chromosomes of this closest assembled relative are distributed among multiple chromosomes in *G. spurium*. For example, genes from *C. laevipes*'s chromosome 3 (cl03) are distributed among five of *G. spurium*'s chromosomes with multiple reciprocal translocations required to explain the current structure. This indicates that although the genome has strong synteny across the entirety of some chromosomes (e.g., cl05 [or cc01] and gs06), more information is needed to reconstruct the evolution of *G. spurium*'s current chromosome structure. Comparison with other genomes in

Galium or *Asperula* would likely be informative for understanding chromosome evolution of *G. spurium*.

Population Genetics

The overall nucleotide diversity (π), the average number of pairwise differences between individuals, averaged 3×10^{-4} . Across all populations, 83% of individuals were homozygous for the major allele, and 16% were homozygous for the minor allele (Figure 7A). Populations had low observed heterozygosity (H_O) with a value of 0.02 overall (Figure 7B). The F_{ST} for the populations was 0.54, with pairwise values ranging from 0.15 to 0.79 (Figure 7C), indicating strong population differentiation (Conner and Hartl 2004), and there were many more homozygotes ($F_{IS} = 0.86$) in the population than expected given random mating. Overall, Provesti's genetic distance between individuals averaged 0.23. The number of alleles that were identical by state and shared between two individuals within a population averaged 88%, and the values were only a little lower (75%) when individuals from different populations were compared. This level of genetic diversity and homozygosity is most similar to that of the germplasm of genetically depauperate crop species. For example, nucleotide diversity was found to be $\pi = 2.3 \times 10^{-4}$ for 736 accessions of coffee (*C. arabica*) (compare with lower-ploidy ancestors: *C. canephora* $\pi = 2.6 \times 10^{-3}$ and *Coffea eugenioides* S. Moore $\pi = 1.1 \times 10^{-3}$), major allelic

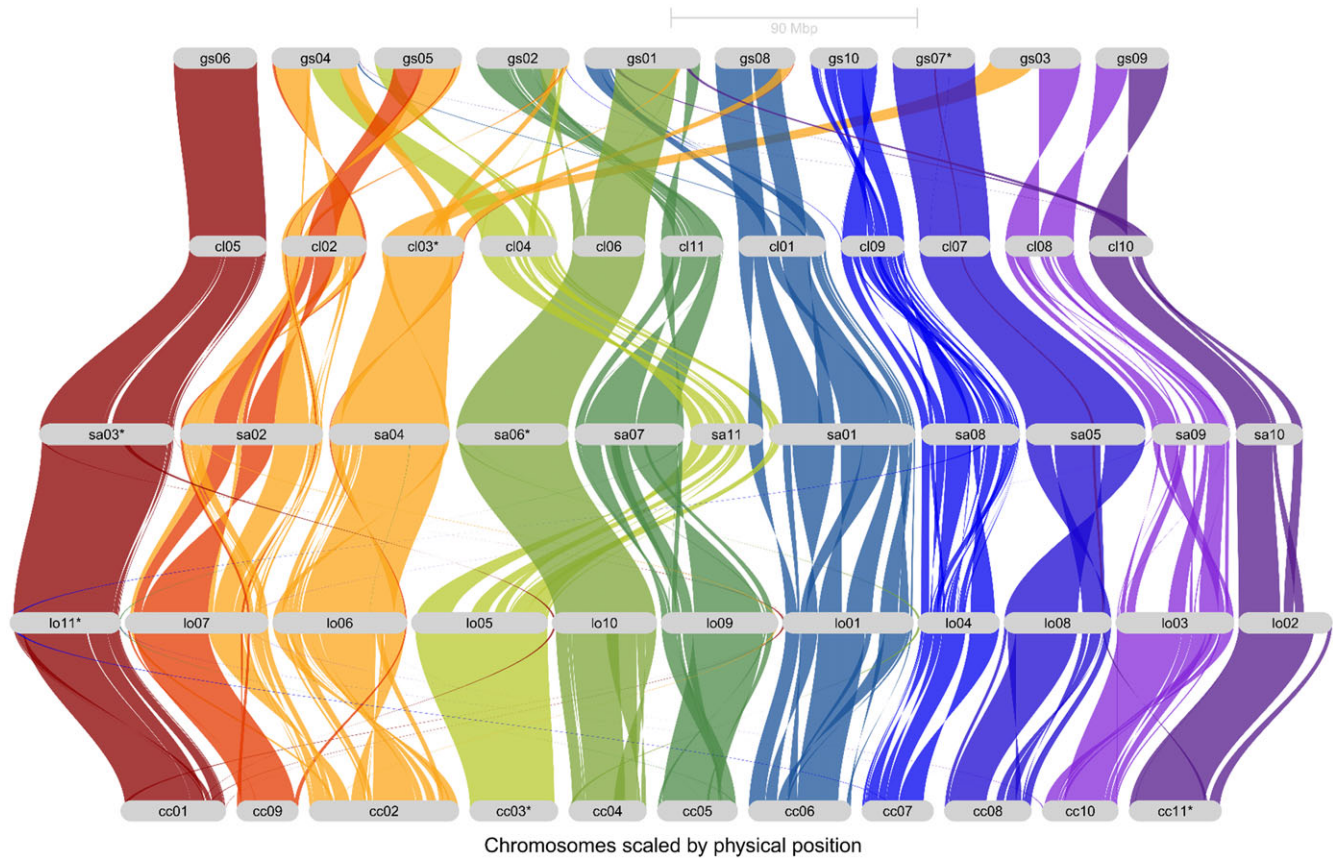


Figure 5. A riparian plot of syntenic relationships among species from the Rubiaceae generated by GENESPACE showing genomic structure across the family, with *Coffea canephora* at the bottom and working upward: *Leptodermis oblonga*, *Sherardia arvensis*, *Cruciata laevipes*, and finally *Galium spurium* at the top of the plot. Asterisks indicate that the chromosome was inverted to clarify the plot. Note that *C. canephora*'s cc09 has been shifted to better indicate its position within the chromosomes of the Rubiaceae species.

frequencies that were largely greater than 95% and a deficiency of heterozygotes—likely a result of reductions in diversity following an origin involving a single allopolyploidization event (Scalabrini et al. 2020). The level of heterozygosity in *G. spurium* is similar to that of 376 tea accessions [*Camellia sinensis* (L.) Kuntze] from the Rwebitaba Tea Research Centre that had an H_O of 0.06 (Tadeo et al. 2024) and 31 accessions of peanut (*Arachis hypogaea* L.) from Taiwan that had major allelic frequencies of 0.87 and an average genetic distance of 0.17. This suggests a high rate of self-fertilization, inbreeding, low gene flow among populations, and low genetic diversity.

This high level of population structure and inbreeding has likely contributed to the relatively slow spread of ALS-inhibitor and quinclorac resistance across the Canadian Prairies. For example, the rate of spread of ALS-inhibitor, glyphosate, or auxinic herbicide resistance in the wind-pollinated, outcrossing species kochia [*Bassia scoparia* (L.) A. J. Scott] with low population structure ($F_{ST} = 0.01$) (Martin et al. 2020) has been rapid, increasing from 4% of sampled sites (Hall et al. 2014) to 78% of sites in 10 yr (Geddes et al. 2023). In contrast, ALS inhibitor-resistant *Galium* was first documented in 1996 in Alberta, Canada (Hall et al. 1998); field surveys from 2007 to 2011 and then 2012 to 2017 found increases in Alberta from 17% to 44%, but lower, more constant levels in Saskatchewan (20%) and Manitoba (17%) (Beckie et al. 2013, 2020). The structured nature of these populations is also reflected in (1) a significant Mantel test indicating a correlation ($P < 0.001$) between geographic distance

and Provesti's genetic distance (dist.genpop::adegenet; Figure 8), (2) 55% of the variation being explained by population (44% by individual) in an analysis of molecular variance, and (3) the clumping of populations as visualized in the principal component analysis of molecular variation (Figure 9). The low genetic diversity of these populations may also limit the potential of the populations to evolve resistances in response to selection from herbicides without recruiting additional variation from processes such as mutation, hybridization, and polyploidization.

Phenotype

A striking aspect of *G. spurium* populations in the field is the level of morphological variation observed. In the common greenhouse environment, while the characteristics we measured showed significant variation, the majority of the populations were statistically equivalent (Figures 10 and 11). A total of 384 plants were included in the common garden greenhouse experiment, with 19 to 22 individuals representing each of the 19 populations. All accessions had the morphological characteristics expected for *G. spurium*, specifically green flowers and small seeds (mericarps), rather than the expected morphological characteristics for *G. aparine* of white flowers and larger mericarps. Some individuals from one accession were shorter, with little distance between internodes and narrower leaves giving them a shorter "mossy" habit; however, the flowers, mericarps, and DNA content were all consistent with the other individuals grown here, and other

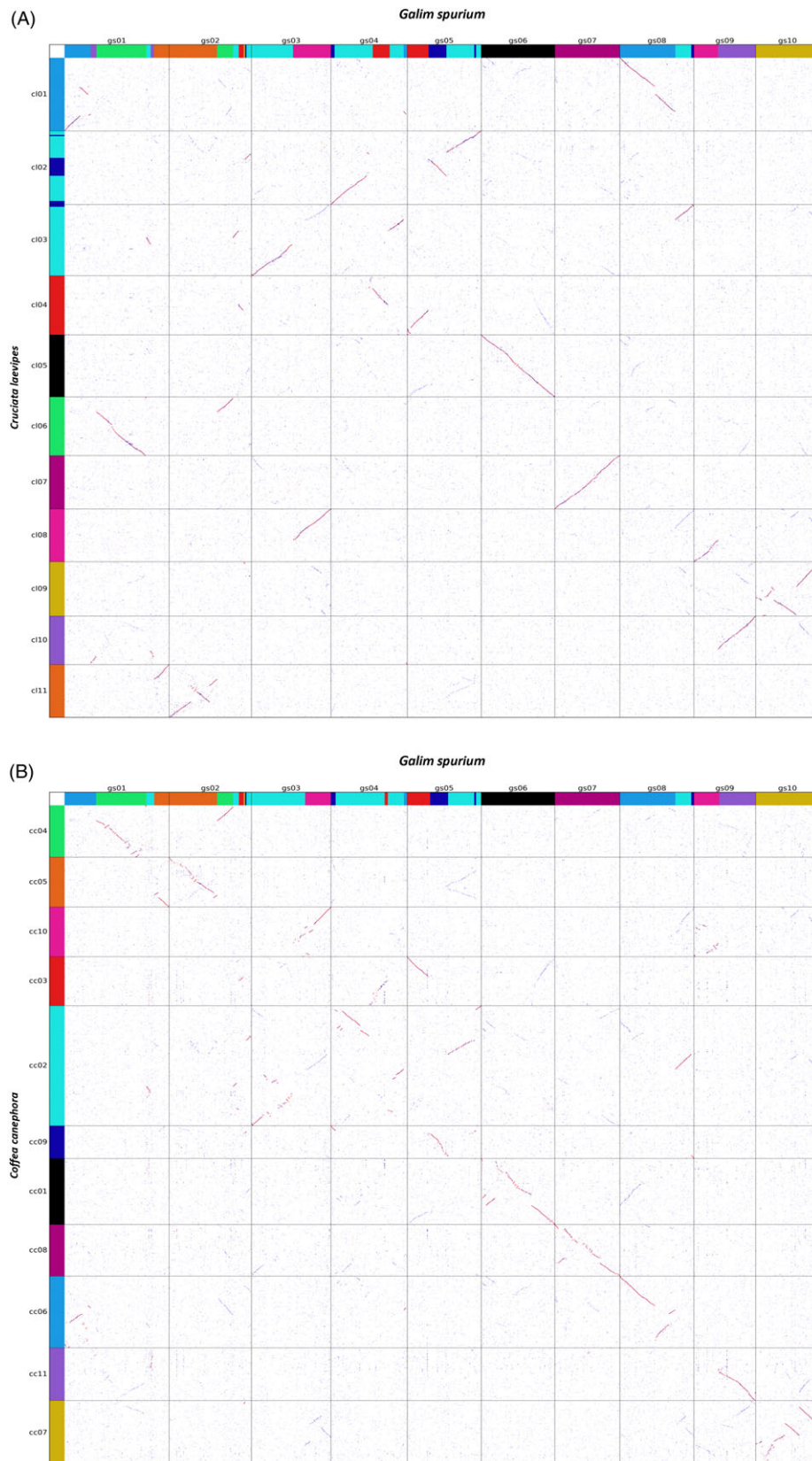


Figure 6. Plots of synteny between proteins of *Galium spurium* and (A) *Cruciate laevipes* and (B) *Coffea canephora*. Red dots indicate the best syntenic matches and blue dots indicate secondary matches, with gray dots indicating lower-order matches. For *G. spurium* and *C. laevipes*, chromosomes are colored based on syntenic relationships with *C. canephora*. We see from these plots that several chromosomes are almost entirely syntenic (e.g., gs06, gs07, and gs10), but there is no clear pattern suggesting that end-to-end joining or nested chromosome fusion led to the reduction in chromosome number in *G. spurium* from $n = 11$ to $n = 10$.

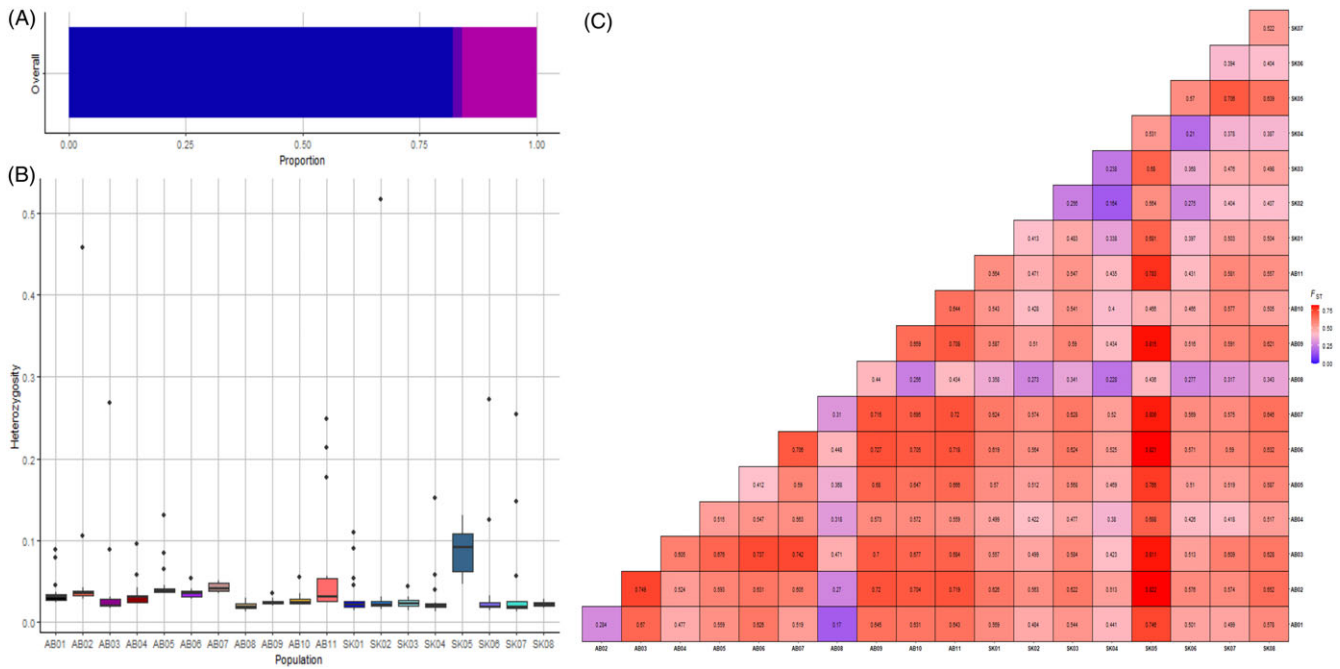


Figure 7. For the 19 populations studied here (A) overall proportion of individuals showing homozygosity for the major allele (blue), heterozygosity (purple), and homozygosity (magenta) for the minor allele; (B) levels of heterozygosity by population; and (C) a heat map of pairwise F_{ST} values for with cooler colors indicating lower F_{ST} values and warmer indicating higher F_{ST} values. Heterozygosity was low across all populations with the majority of individuals (83%) homozygous for the reference allele with evidence of limited outcrossing. On average, the F_{ST} values were 0.54, but AB-08 showed lower pairwise F_{ST} values across comparisons and SK-05 showed higher values.

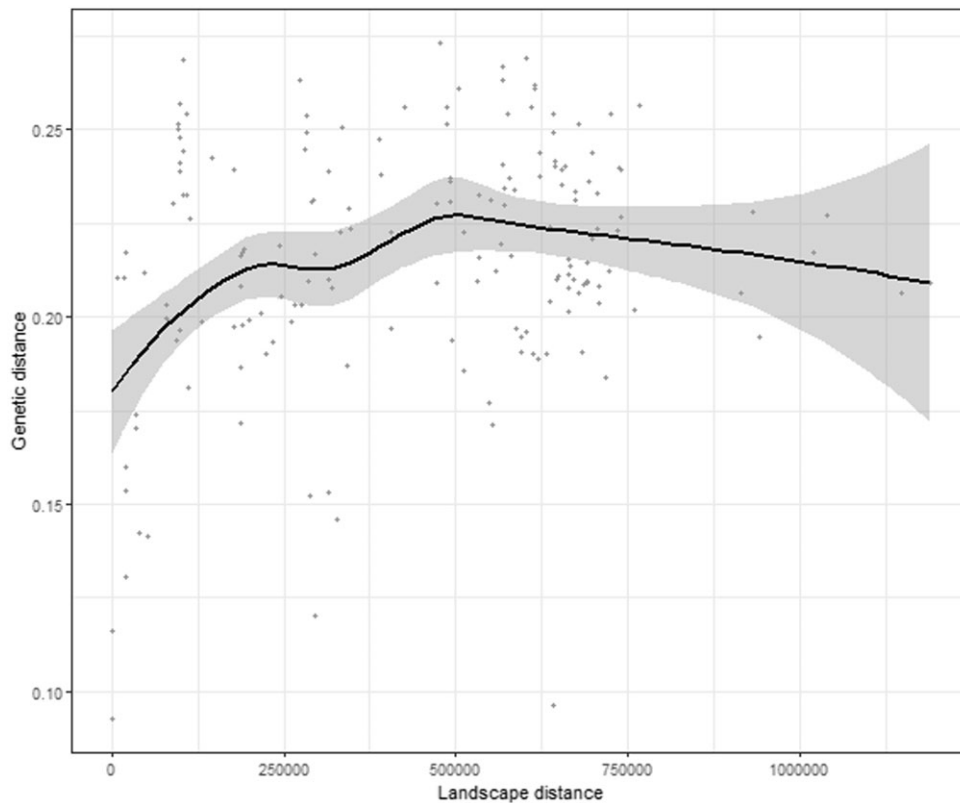


Figure 8. Provesti's genetic distance (y axis) by geographic (landscape) distance (m) for pairings of the 19 populations. This graph (graph41g::scatter_dist) shows a smooth (loess) line with 95% confidence interval. A Mantel test with 1,000 Monte Carlo repetitions indicates a significant ($P < 0.001$) positive relationship providing evidence of isolation by distance.

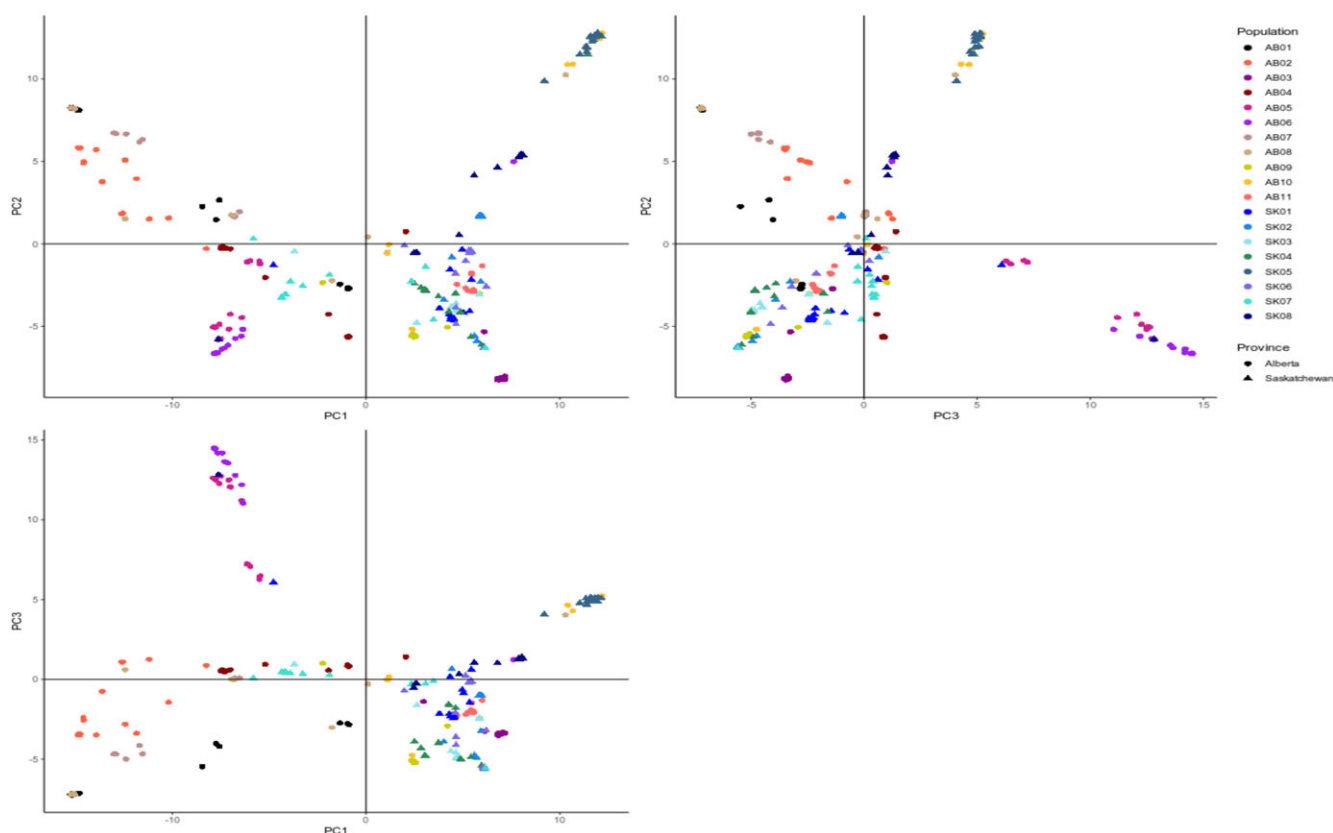


Figure 9. Principal component analysis (PCA) of the genetic variation of single-nucleotide polymorphism (SNP) data. Circles in warm colors represent individuals from Alberta and triangles in cool colors represent those from Saskatchewan. Clumping of individuals from the same population is evident, but variation among populations provides spread. Axis 1 explains 76% of the variation, while axis 2 explains 44%.

members of the same accession had more typical morphology, suggesting this is part of the variation for the species.

In the germination experiment, 51% of the seeds (20 per population) on average had emerged after 7 d (Figure 10A). Variation was seen by population, with AB-06 showing faster germination (90%) than 10 other populations including the slowest to germinate SK-08 (15%), but most populations showed overlapping confidence intervals and were not statistically different because of high variability. At 6 wk after planting, an average of 43% of the plants had begun flowering (Figure 10B). Again, there was statistically significant variation among populations, with AB-02 and AB-06 having significantly more flowering individuals than 13 populations, including AB-09, AB-10, or SK-08, but most of the populations were not statistically different. Similarly, after 8 wk, at the end of the greenhouse experiment, the majority of populations had a high proportion of plants that had set seed (79%), and while population AB-10 had statistically fewer plants with seed than most other populations, most populations were not statistically distinct (Figure 10C).

The morphological characteristics measured showed less variation than the phenological characteristics, but they still showed a few statistical differences overall. The average height of the plants at 8 wk was 107.2 cm, with the tallest population, AB-04, averaging 132.0 cm, and the shortest, AB-10, averaging less than half of this at 53.8 cm (Figure 11A). Total estimated seed production averaged 3,158, with AB-01 and SK-01 producing the most seed (more than 3,500 seeds each), and AB-10 producing the least with half of this amount (1,720; Figure 11B). Average

diameter of a mericarp was 1.8 mm, with the populations with the largest mericarps, such as AB-04 (2.04 mm), statistically different from the populations with the smallest mericarps SK-06 (1.54 mm); (Figure 11C). However, as with germination, flowering, and seed production, the majority of populations were not statistically different from each other for height, total seed production, or seed size. Flower size did not differ statistically across populations and averaged 1.9 mm (0.18 mm standard deviation).

A redundancy analysis (RDA) was used to investigate the association between genotype and the phenotype observed in the greenhouse. Five characteristics measured in the greenhouse were retained for the analysis after eliminating continuous variables that had strong correlation to each other and factors that had too few individuals in each category. The retained characteristics were height and flowering status at 4 wk, total plant weight, seed count, and the density of hooks on the mericarp. The RDA indicated these predictors explained (R^2) 5.5% of the variation in the data after adjustment, and the model was significant according to a permutation test (1,000; $P < 0.001$). A total of 34 candidate SNPs with RDA loadings 3 SDs or more from the center of their distributions were examined. This minimized false-positive rates for SNPs of interest by setting the two-tailed P -value at 0.0027. Of these 34 SNPs, the majority (24) were associated with the density of hooks of the mericarp (Figures 2 and 12). Among the remaining SNPs with high loadings, nine were associated with total plant weight at harvest and one with early flowering time. This indicates that the majority of these SNPs are likely to be under selection as a result of association with

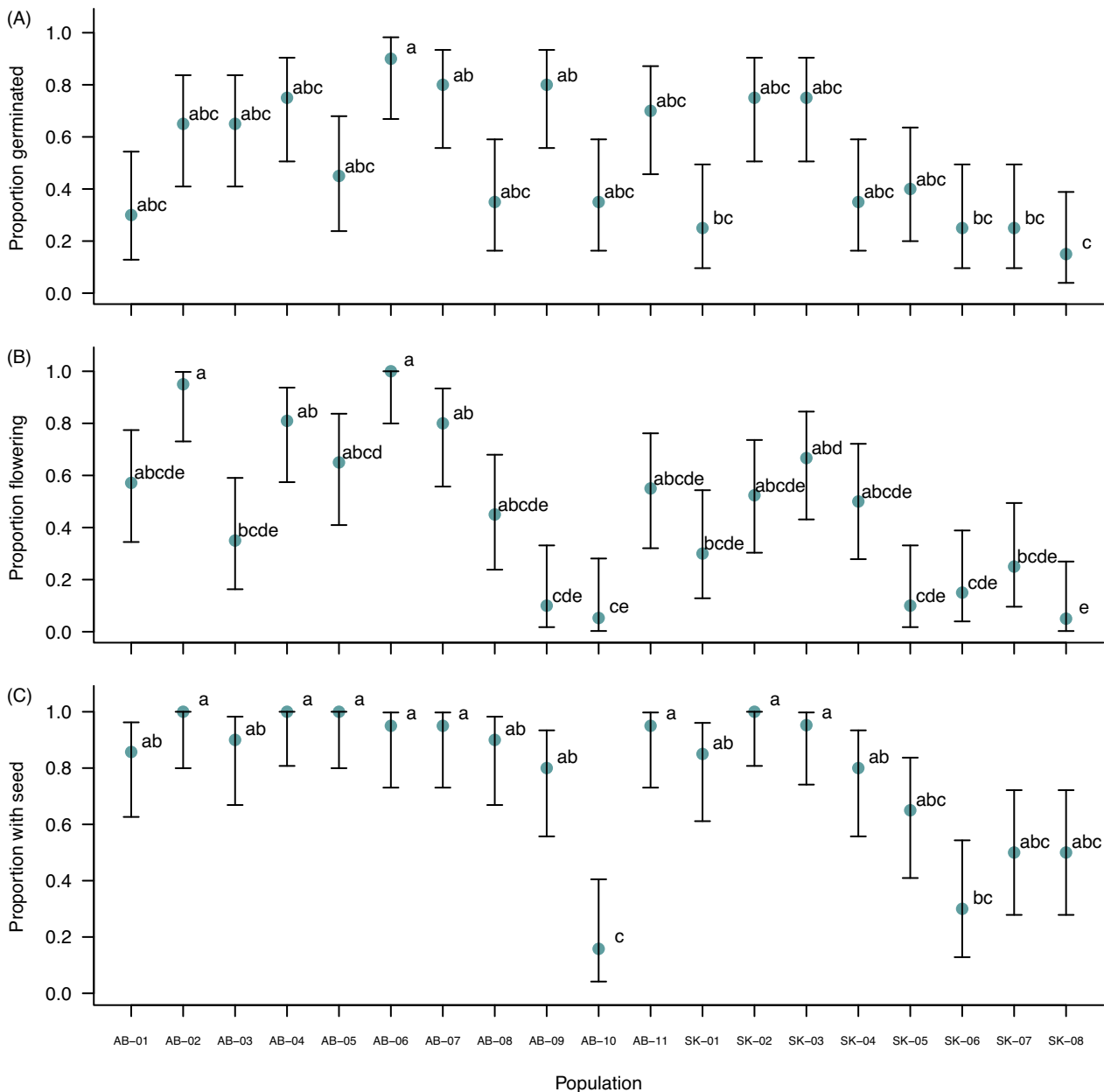


Figure 10. Phenological data from the 19 populations grown in the greenhouse, including (A) proportion of seed germinated after 7 d, (B) proportion flowering at 6 wk, and (C) proportion of plants with seed at 8 wk. In all cases, statistical differences are observed, but the majority of populations are highly variable and show strong overlap with values from the other populations.

the density of hooks on their mericarps. Individuals that were scored as without hooks or with a low density of hooks occurred sporadically across the populations, but were most frequent in populations SK06, SK07, and SK08 (Figures 1 and 2). Variation in the density of spines on the mericarps of *G. spurium*, has been previously described and used to separate individuals into two forms: *G. spurium* f. *spurium* with smooth fruit, and *G. spurium* f. *vaillantii* with hooked spines (Moore 1975). Moore (1975) indicates that Linnaeus's specimen of the species was the smooth form, but that the smooth form was less common in the material examined from the Canadian Prairies. Further, he noted that one of the two sites with smooth-form specimens was near Melfort, SK, close to where our populations with the most smooth-fruited individuals were collected. Malik and Vanden Born (1988) noted

that they observed an intermediate variant in material from Alberta and Saskatchewan and that the presence of more than one form in a field was common. The presence of the hooked spines on the mericarp are inferred to provide an advantage for dispersal by animals (Malik and Vanden Born 1988). More work is needed to understand the genetic basis of hooks on these fruits and how the character influences the fitness of these populations, but the species may offer an excellent opportunity for this work, as the development of nearly isogenic lines that differ for this character should be possible.

The data from the common environment, combined with the result of the population genetics presented earlier, suggest that some of the disjunct morphological variation observed within populations is likely the result of a combination of the inbred

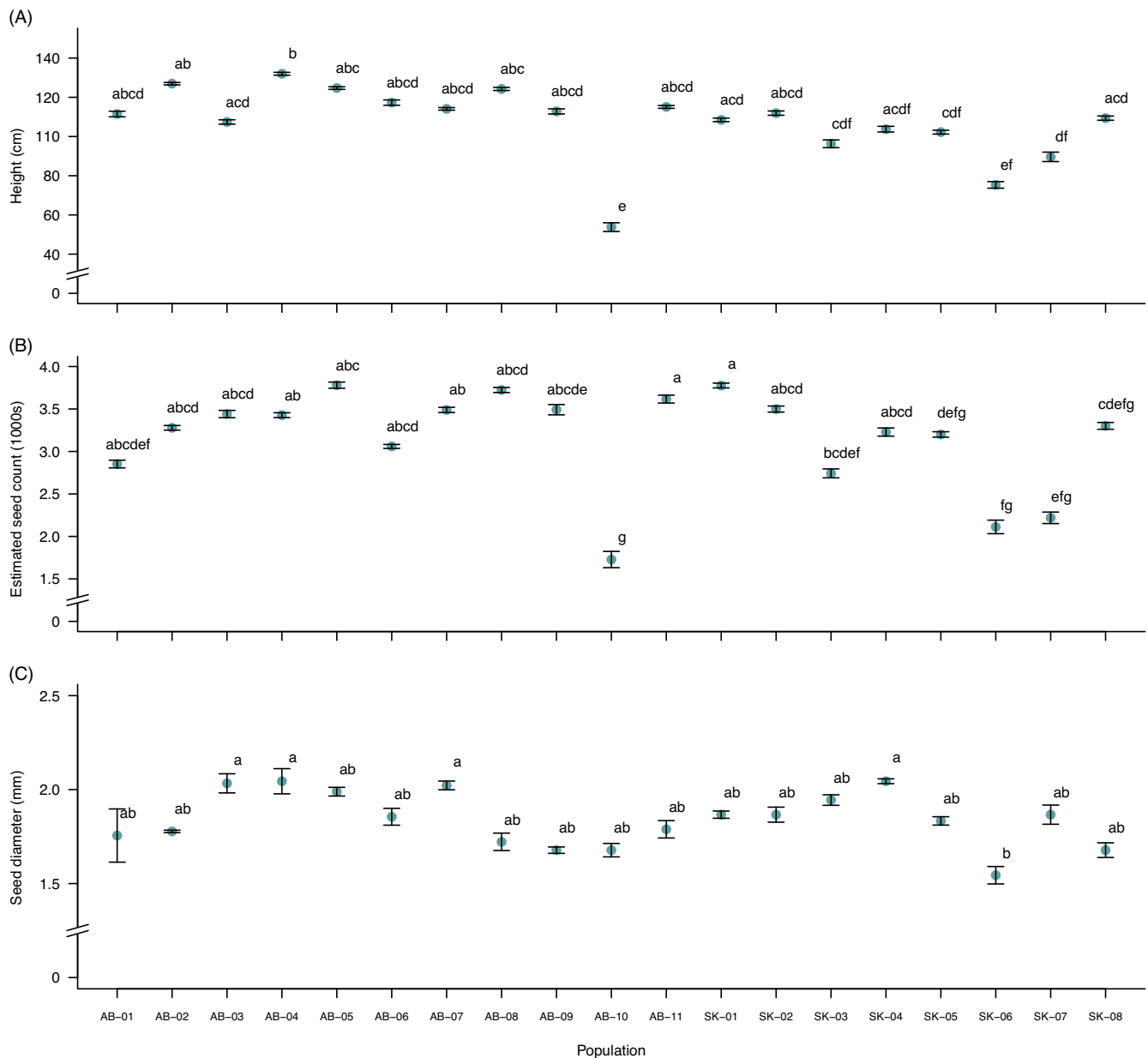


Figure 11. Morphological data from the 19 populations grown in the greenhouse for key characteristics, including (A) plant height at 6 wk, (B) total estimated seed count, and (C) seed (mericarp) diameter.

nature of groups of individuals observed within the same field and environmentally induced variation. Differences among individuals in a field, such as a lack of hooks on the mericarp, likely reflects homozygosity for an alternative allele. However, given the minimal amount of genetic variation observed overall and the strong genetic similarity among samples even from different populations, much of the variation in characteristics such as emergence and flowering time is likely attributable to environmental variation, given differing conditions rather than genetic differences.

Potential and Selection Herbicide-Resistance Genes

Management of *G. spurius* in western Canadian crops has been primarily reliant on herbicides from the following modes of action: ALS inhibitors (Group 2), synthetic auxins (Group 4),

5-enolpyruvylshikimate-3-phosphate synthase (EPSPS) inhibitors (Group 9), glutamine synthetase inhibitors (Group 10), and more recently, protoporphyrinogen oxidase (PPO) inhibitors (Group 14) and 4-hydroxyphenylpyruvate dioxygenase (HPPD) inhibitors (Group 27) (Anonymous 2022). In some crops, such as some pulse crops, the ALS-inhibiting herbicides are nearly the only option. Resistance to ALS inhibitors has spread through the populations of *G. spurius* on the Canadian Prairies, although it has not yet reached fixation (Beckie et al. 2020). The ALS proteins from *G. aparine* and *C. arabica* mapped to *G. spurius*'s chromosome gs06. The amino acid sequence captured in this genome assembly has one of the point mutations, Trp-574-Leu, reported to confer ALS-inhibitor resistance in *G. aparine* by Deng et al. (2019). No changes are observed at residue Pro-197 or Asp-376, which are the two other sites Deng et al. (2019) reported to confer ALS-inhibitor resistance in *G. aparine*. Two other changes in the amino acid

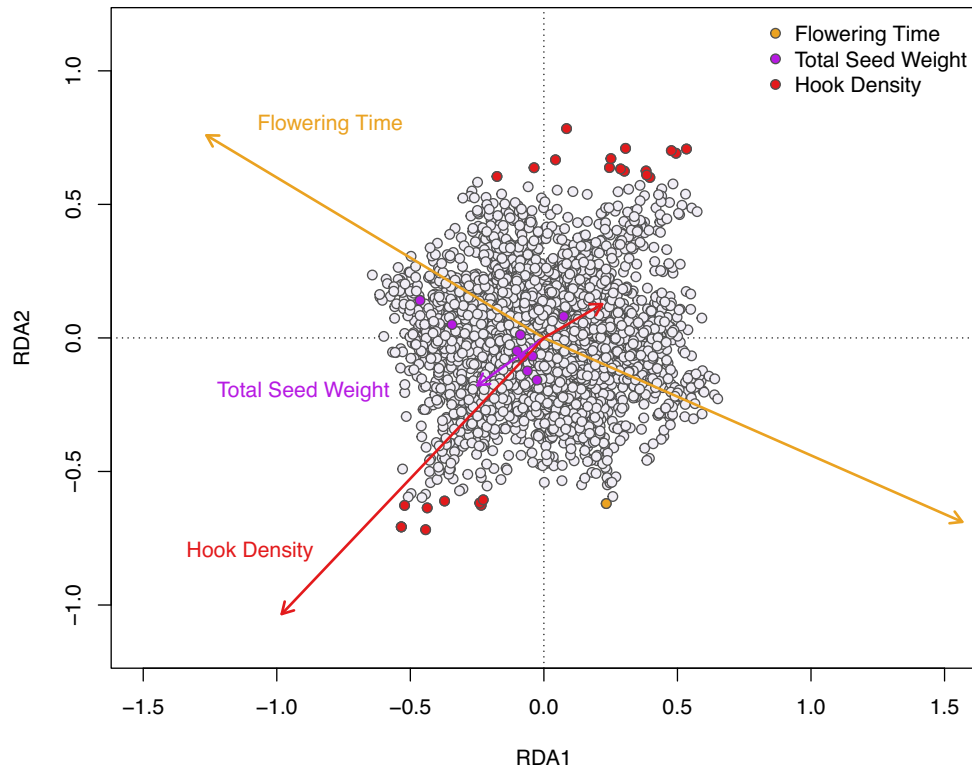


Figure 12. Redundancy analysis (RDA) examining how variation in the single-nucleotide polymorphism (SNP) data is associated with variation in key traits. A total of 5.5% of the variation in the SNP data was explained by the morphological characteristics included. The majority of highly loading SNPs (70%), with a cutoff of 3 SDs from the mean, were associated with hook density and are highlighted in red. Most of the remaining SNPs are associated with total seed weight (26%) and highlighted in purple, while the one SNP associated with flowering time is in yellow.

sequence are present compared with the susceptible sequence in GenBank (Sun et al. 2011): Thr-59-Ala and Ala-380-Thr, but these sites do not correspond to any of the other sites (Ala-122, Ala-205, Arg-377, Ser-653, or Gly-654) reported to confer resistance in other weed species (Tranel et al. 2023). We used the R package PCADAPT to detect SNPs under selection and compared them with the location of the genes of interest (Luu et al. 2017; Privé et al. 2020). Five principal components were chosen based on the scree plot, and alpha was set to 0.01 for a false discovery rate of 1:100 after correction with the Benjamini-Hochberg procedure. The SNPs were thinned to reduce the effect of linkage disequilibrium, with size set to 200, threshold set to 0.1, and the minimum minor allelic frequency set to 2%. A total of 192 SNPs were identified as outliers, and their position was compared with the position of the genes of interest for involvement in herbicide resistance (Figure 13; Table 2; Supplementary Table 4). Two outlying SNPs were found within 0.5 Mbp of the *ALS* gene on *gs06*, a potential indication of the selection on the locus that is occurring with the ongoing spread of the *ALS*-inhibitor resistance.

In contrast to *ALS*-inhibitor resistance, resistance to quinclorac, a synthetic auxin, has not yet become widespread in these populations (Beckie et al. 2020; Van Eerd 2004; Van Eerd et al. 2004), although surveying has been limited. There has been a lower global incidence of synthetic auxin herbicide resistance compared with *ALS*-inhibitor resistance (Heap 2023). This is likely a consequence of the importance of auxin, which should be viewed not as a hormone, but as an ancient, complex, connective, impetus signal with self-organizing transport streams of indole-3-acetic acid (IAA) (Zažimalová et al. 2014). The target site of synthetic auxins such as quinclorac is still being elucidated, with the

complexity, flexibility, and redundancy of the auxin pathway complicating our understanding of both its normal and abnormal functioning (Todd et al. 2020; Zažimalová et al. 2010). Synthetic auxins in susceptible plants are highly stable IAA mimics that lead to an “auxin overdose” (Grossmann 2010). The cause of demise in *G. spurium* is suspected to be the production and accumulation of reactive oxygen species, including hydrogen peroxide, and resistance, controlled by a recessive nuclear gene, has been hypothesized to be the result of a mutation at a target site or along the signal transduction pathway (Van Eerd et al. 2005).

One critical auxin receptor is TIR1, an F-box protein found in the nucleus (Dharmasiri et al. 2005a; Kepinski and Leyser 2005). Auxins regulates gene expression by acting as “molecular glue,” filling the cavity between TIR1 and the substrate by forming a continuous hydrophobic core (Tan et al. 2007). Multiple homologues of TIR1 have been identified (Dharmasiri et al. 2005b) and *Arabidopsis* mutants for auxin signaling F-box protein 5 (AFB5) have demonstrated differential resistance to picolinic acids (picloram, clopyralid) but no other synthetic auxins (Walsh et al. 2006). TIR1/AFB is the substrate recognition subunit of SCF^{TIR1/AFB}, an E3 ubiquitin ligase complex that catalyzes the conjugation of ubiquitin to Aux/IAA repressor proteins, which then is targeted by the 26S proteasome for degradation (Quint and Gray 2006). Once the AUX/IAA repressor proteins are degraded, auxin response factor (ARF) transcription factors can bind to auxin-responsive genes in the DNA (Li et al. 2016).

The herbicide 2,4-D was found to similarly influence the binding pocket of TIR1 as IAA, which promotes SCF ubiquitin ligase-catalyzed degradation of AUX/IAA (Tan et al. 2007). Transcription of acetyl-CoA carboxylase ACC synthase (ACS)

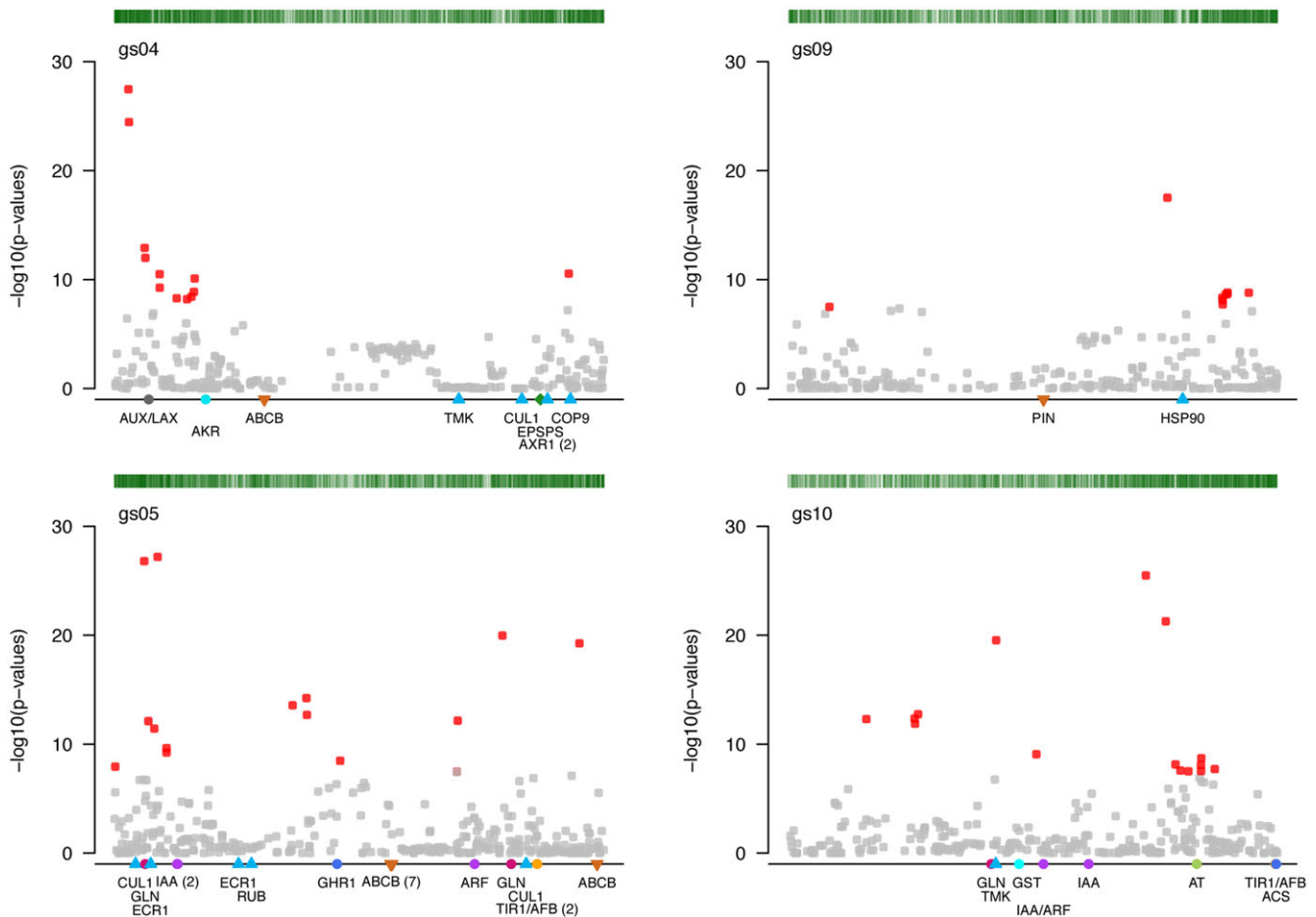


Figure 13. (Continued).

staging, whereby mature tissue was more tolerant than reproductively immature tissue.

In their recent review, Todd et al. (2020) suggest that target-site mutations in auxin perception and signaling could involve three major groups of auxin signaling proteins: (1) auxin efflux and influx transporters (PIN, ABCB, AUX/LAX); (2) auxin perception and signaling proteins: ARFs, transcriptional repressors (AUX/IAA), and the Skp1-Cullin-F-Box TIR1/AFB ubiquitin ligase complex (AXR1, ECR1, RCF1, HSP90/SGT1, RB, NEDD8, CAND1, COP9, CUL1); and (3) the transmembrane kinase family (TMK). The ARF proteins compete for promoter target sites of auxin response genes and dimerize with AUX/IAA repressor proteins at low auxin concentrations, while when auxin concentrations are high, AUX/IAA repressor proteins interact with TIR1/AFB and the AUX/IAA proteins become ubiquitinated and ultimately degraded via the 26S proteasome pathway (reviewed in Luo et al. 2018). In *Arabidopsis* mutants, loss of TMK activity affected auxin signal transduction in root and potentially shoot development, cell expansion in roots, hypocotyls, and stamen filaments, and leaf cell expansion and cell proliferation (Dai et al. 2013). Additionally, a mutation in the auxin receptor auxin binding protein 1 (ABP1) was identified in Group 4, synthetic auxin-resistant wild mustard (*Sinapis arvensis* L.) from Manitoba (Grossmann 2010; Zheng and Hall 2001).

Multiple homologues for these auxin efflux and influx transporters were identified in the *G. spurium* genome: 4 of the PIN-FORMED auxin efflux carrier protein (PIN1), 3 of the AUXIN1/LIKE-AUX1 (AUX/LAX) auxin influx carrier proteins, and 13 of the ATP-binding cassette B (ABCB) proteins (Supplementary Table 5). Nine proteins with homology to the transcriptional repressors (IAA), nine with homology to ARFs, and six with homology to both were also found (IAA/ARF). Five homologues of TIR1/AFB were found and at least one homologue of most of the genes involved in the formation of the Skp1-Cullin-F-Box TIR1/AFB E3 ubiquitin ligase complex were located, as was one homologue of ABP1 (Supplementary Table 5). Four homologues of TMK were also located. We note that the annotation of the genome will not be complete, as there will be genes that were not expressed in the rosette at the stage or which have not been annotated correctly by the pipeline. Additional RNA work could improve these annotations and may indicate additional homologues.

Fifteen genes associated with synthetic auxin resistance (Group 4) (Table 2; Figure 13) are among the top 20 gene homologues with known or potential roles in herbicide resistance that contain SNPs identified as likely under selection within 1 Mbp. This includes nine genes associated with auxin perception: (1) five outlying SNPs of a AUX/IAA repressor protein homologue on gs06; (2) four SNPs each near CAND1 and ERC1 (components for

Table 2. Top 20 homologues of genes with known or potential roles in herbicide resistance ranked by proximity to single-nucleotide polymorphisms (SNPs) under selection.^a

Homologue	Putative role	Chromosome	Gene name	Nearest SNP distance bp	SNPs within 1 Mbp
AT	Alpha tubulin	gs08	GS3201901	19,783	6
IAA	Auxin-induced gene	gs06	GS2558401	11,751	5
AUX/LAX	Auxin influx transporter	gs08	GS3259201	26,589	4
AT	Alpha tubulin	gs10	GS0705701	212,913	4
CAND1	Cullin-associated and neddylation-dissociated	gs02	GS1201501	79,948	4
ECR1	RUB-activating enzyme	gs05	GS1976901	151,288	4
ARF	Auxin response factor	gs08	GS2988101	43,412	3
AUX/LAX	Auxin influx carrier	gs04	GS1619901	218,631	2
GLN	Glutamine synthetase	gs05	GS1972001	61,194	2
TMK	Transmembrane kinase	gs08	GS3026001	18,963	2
ABCB	ATP-binding cassette B	gs06	GS2393501	93,165	2
ALS	Acetolactate synthase	gs06	GS2530401	312,834	2
ABP1	Auxin binding protein	gs06	GS2594801	85,962	2
ARF	Auxin response factor	gs02	GS1185401	491,484	1
IAA/ARF	Auxin-induced gene	gs08	GS3157301	497,879	1
TIR/AFB	Auxin receptor	gs06	GS2589801	381,117	1
PIN	Auxin efflux carrier	gs01	GS0071401	316,058	1
IAA	Auxin-induced gene	gs01	GS0066501	174,697	1
GLN	Glutamine synthetase	gs01	GS0176201	66,200	1
PIN	Auxin efflux carrier	gs01	GS0181001	485,054	1

^aColumns contain information on the homologue, the gene's position in the genome, the distance to the nearest SNP indicating selection, and the number of these SNPs within a 1-Mbp window centered on the gene's midpoint. See Supplementary Table 4 for all results. SNPs were identified as under selection using ordination with almost 4,000 SNPs across the genome included. The Benjamini-Hochberg procedure was used to adjust significance value to control false discovery, which was set to 1%. SNPs were thinned to reduce the effects of linkage disequilibrium.

Skp1-Cullin-F-Box TIR1/AFB E3 ubiquitin ligase complex) on gs02 and gs05, respectively; (3) three SNPs close to an ARF homologue on gs08; (4) one SNP near ARF on gs02; (5) one SNP near IAA/ARF on gs08; (6) one SNP near TIR/AFB on gs06; and (7) one SNP near AUX/IAA on gs01 (Table 2). For auxin transport genes, five homologues were identified: (1) four SNPs were found close to the auxin influx transporter (AUX/LAX) gene on gs08, (2) two SNPs were found close to AUX/LAX on gs04, (3) two SNPs were located near ABCB on gs06, (4) one SNP was found near a PIN homologue on gs01, and (5) another SNP was found near a second PIN homologue on gs01. Finally, two SNPs were located near the TMK gene on gs08 and two SNPs were located near ABP1 on gs06 (Table 2). SNPs showing evidence of selection are not necessarily contained in a gene under selection, but rather can be linked to nearby genes under selection. This means that while this analysis indicates regions of the genome where selection is occurring, the region contains numerous genes, making conclusive determinations that selection is occurring on a specific gene impossible, and we cannot determine what is causing that selection. More specifically, an SNP showing strong selection near known herbicide-resistant genes could be indicative of selection on that gene or on other nearby genes and may or may not be related to the evolution of herbicide resistance. As a result, while these SNPs cannot be conclusively attributed to selection on these genes, they can motivate further more targeted research, such as differential expression analysis in herbicide-resistant and herbicide-susceptible individuals. This chromosome-level assembly provides a fundamental resource for this analysis.

One or two homologues of the genes targeted by the remaining herbicides used to control *G. spurium* (EPSPS inhibitors, S-glutamine synthetase inhibitors, PPO inhibitors, and HPPD inhibitors; Anonymous 2022) were also found in the assembly. The predicted EPSPS protein was found as a single copy on gs04 and, as expected from a lack of reported resistance, did not show evidence of carrying a point mutation at Thr-102, Ala-103, or Pro-106 (Gaines and Heap 2023). A single homologue of

protoporphyrinogen oxidase 2 (PPO2) was identified on gs02. The amino acids where changes are reported to potentially confer PPO2 resistance (Asn-98, Arg-128, Gly-383, Leu-385, Leu-398, Gly-399, Tyr-400, Leu-401, and Phe-421) are all conserved in this genome sequence (Rangani et al. 2019). Two glutamine synthetase homologues were identified on gs03 and gs10, each with a single candidate SNP within 1 Mbp of their positions. A single homologue of HPPD was identified on gs02; however, while *Amaranthus* spp. and wild radish (*Raphanus raphanistrum* L.) have evolved HPPD resistance, the mechanism for this resistance appears to be a change in the plant's metabolism or the gene's expression pattern rather than point mutations in the target site (Lu et al. 2020; Nakka et al. 2017).

Two of the genes with the highest number of SNPs in the vicinity are the two of the four homologues of alpha-tubulin genes TOR2 and TUA5 located on gs08 and gs10. Alpha-tubulins are the target of Group 3, dinitroaniline herbicides such as trifluralin and ethalfluralin. While trifluralin does not control *G. spurium* and ethalfluralin only provides suppression (Anonymous 2022), it is possible the species is exposed to these microtubule inhibitors when other species are the primary targets for control. Point mutations at six sites in the alpha-tubulin genes have been determined to be the source of Group 3 resistance in grass species: goosegrass [*Eleusine indica* (L.) Gaertn.] (Anthony et al. 1998; Yamamoto et al. 1998), green foxtail [*Setaria viridis* (L.) P. Beauv.] (Délye et al. 2004), shortawn foxtail (*Alopecurus aequalis* Sobol.) (Hashim et al. 2012), and rigid ryegrass (*Lolium rigidum* Gaudin) (Chu et al. 2018). None of these point mutations are represented in our draft genome, and these genes are involved in fundamental processes such as successful mitosis and movement of organelles (Ludwig et al. 1987), so it is entirely possible that selection on these genes, if it is occurring, is unrelated to herbicide resistance.

Here we have produced a reference-quality, chromosome-level assembly for *G. spurium* and compared the genome with its nearest relatives with similar information available. We note that the currently sequenced genomes with $n = 11$ in the family show

relative stability, but there is no clear mechanism that caused the reduction to $n = 10$ in *G. spurium*, given the available genomes. The ddRAD-tag data for the 19 Canadian Prairie populations indicate very low heterozygosity and high inbreeding rates that result in structured populations with limited gene flow. This likely explains the relatively slow movement of herbicide resistance genes in these populations. This work also indicates some gene candidates of interest that may be involved in the evolution of auxinic resistance in this species. These can be targeted for further investigation and include the *IAA* gene on chromosome 6 and the *AUX* gene on chromosome 8. The availability of the *G. spurium* genome will facilitate future research into the genetic basis of auxin resistance in the species and systematics research into the polyphyletic genus *Galium*.

Supplementary material. To view supplementary material for this article, please visit <https://doi.org/10.1017/wsc.2024.79>

Acknowledgments. We would like to thank the ORDC greenhouse staff for their help in growing the plants for this work; Taylor Withey for counting, measuring, and photographing the seeds produced during the greenhouse trial; and Shefali Vishwakarma for initial work on the RAD-seq files in STACKS. We would also like to thank Dr. Martin Laforest for suggestions on which genes to include in the list of interest for the evolution of herbicide resistance.

Funding statement. This work was funded by Agriculture and Agri-Food Canada through the Agricultural Plant Systematics Project (J-002275).

Competing interests. The authors declare no conflicts of interest.

References

- Anonymous (2022) 2022 Guide to Crop Protection. Regina: Saskatchewan Ministry of Agriculture. 36 p
- Anthony RG, Waldin TR, Ray JA, Bright SWJ, Hussey PJ (1998) Herbicide resistance caused by spontaneous mutation of the cytoskeletal protein tubulin. *Nature* 393:260–263
- Bache SM, Wickham H (2022) magrittr: A Forward-Pipe Operator for R. R Package Version 2.0.3. <https://magrittr.tidyverse.org/>. Accessed: Nov 1, 2022
- Beckie H, Shirriff S, Leeson J, Hall L, Harker K, Dokken-Bouchard FB, Brenzil CA (2020) Herbicide-resistant weeds in the Canadian prairies: 2012 to 2017. *Weed Technol* 34:461–474
- Beckie HJ, Lozinski C, Shirriff S, Brenzil CA (2013) Herbicide-resistant weeds in the Canadian prairies: 2007 to 2011. *Weed Technol* 27:171–183
- Beckie HJ, Warwick SI, Sauder CA, Kelln GM, Lozinski C (2012) Acetolactate synthase inhibitor-resistant *Galium spurium* in western Canada. *Weed Technol* 26:151–155
- Bodenhofer U, Bonatesta E, Horejs-Kainrath C, Hochreiter S (2015) msa: an R package for multiple sequence alignment. *Bioinformatics* 31:3997–3999
- Bremer B (2009) A review of molecular phylogenetic studies of Rubiaceae. *Ann MO Bot Gard* 96:4–26
- Brownrigg R, Minka TP, Deckman A (2022) maps: Draw Geographical Maps. R Package Version 3.4.1. <https://cran.r-project.org/web/packages/maps/index.html>. Accessed: Nov 1, 2022
- Brůna T, Hoff KJ, Lomsadze A, Stanke M, Borodovsky M (2021) BRAKER2: automatic eukaryotic genome annotation with GeneMark-EP+ and AUGUSTUS supported by a protein database. *NAR Genom Bioinform* 3: lqaa108
- Catchen J, Hohenlohe PA, Bassham S, Amores A, Cresko WA (2013) Stacks: an analysis tool set for population genomics. *Mol Ecol* 22:3124–3140
- Charif D, Lobry JR (2007) Seqin{R} 1.0-2: a contributed package to the {R} project for statistical computing devoted to biological sequences retrieval and analysis. Pages 207–232 in Bastolla U, Porto M, Roman HE, Vendruscolo M, eds. *Structural Approaches to Sequence Evolution: Molecules, Networks, Populations*. New York: Springer
- Chen T, Ehrendorfer F (2001) *Galium*. Pages 104–141 in Committee FoCE, ed. *Flora of China*. http://www.efloras.org/florataxon.aspx?flora_id=2&taxon_id=250090777. Accessed: Jan 6, 2025
- Chen Y, Chen Y, Shi C, Huang Z, Zhang Y, Li S, Li Y, Ye J, Yu C, Li Z, Zhang X, Wang J, Yang H, Fang L, Chen Q (2018) SOAPnuke: a MapReduce acceleration-supported software for integrated quality control and preprocessing of high-throughput sequencing data. *Gigascience* 7:1–6
- Chu Z, Chen J, Nyporko A, Han H, Yu Q, Powles S (2018) Novel alpha-tubulin mutations conferring resistance to dinitroaniline herbicides in *Lolium rigidum*. *Front Plant Sci* 9:97
- Conner JK, Hartl DL (2004) *A Primer of Ecological Genetics*. Sunderland, MA: Sinauer. 304 p
- Dai N, Wang W, Patterson SE, Bleecker AB (2013) The TMK subfamily of receptor-like kinases in *Arabidopsis* display an essential role in growth and a reduced sensitivity to auxin. *PLoS ONE* 8:e60990
- Danecek P, Auton A, Abecasis G, Albers CA, Banks E, DePristo MA, Handsaker RE, Lunter G, Marth GT, Sherry ST, McVean G, Durbin R, 1000 Genomes Project Analysis Group (2011) The variant call format and VCFtools. *Bioinformatics* 27:2156–2158
- Délye C, Menchari Y, Michel S, Darmency H (2004) Molecular bases for sensitivity to tubulin-binding herbicides in green foxtail. *Plant Physiol* 136:3920–3932
- Deng W, Di Y, Cai J, Chen Y, Yuan S (2019) Target site resistance mechanisms to tribenuron-methyl and cross-resistance patterns to ALS-inhibiting herbicides of catchweed bedstraw (*Galium aparine*) with different ALS mutations. *Weed Sci* 67:183–188
- Dharmasiri N, Dharmasiri S, Estelle M (2005a) The F-box protein TIR1 is an auxin receptor. *Nature* 435:441–445
- Dharmasiri N, Dharmasiri S, Weijers D, Lechner E, Yamada M, Hobbie L, Ehrismann JS, Jürgens G, Estelle M (2005b) Plant development is regulated by a family of auxin receptor F-box proteins. *Dev Cell* 9:109–119
- Ellinghaus D, Kurtz S, Willhoeft U (2008) LTRharvest: an efficient and flexible software for de novo detection of LTR retrotransposons. *BMC Bioinformatics* 9:18
- Emms DM, Kelly S (2018) STAG: species tree inference from all genes. *bioRxiv* 10.1101/267914
- Emms DM, Kelly S (2019) OrthoFinder: phylogenetic orthology inference for comparative genomics. *Genome Biol* 20:238
- Flanagan SP (2023) gwscAR: Genome-Wide Selection Components Analysis in R. R Package Version 0.1.0. <https://github.com/spflanagan/gwscAR>. Accessed: Nov 15, 2023
- Fox J, Weisberg S (2019) *An R Companion to Applied Regression*. 3rd ed. Thousand Oaks, CA: Sage. 607 p
- Gaines TA, Heap IM (2023) Mutations in Herbicide-Resistant Weeds to Inhibition of Enolpyruvyl Shikimate Phosphate Synthase. www.weedscience.com. Accessed: August 9, 2023
- Geddes CM, Pittman MM, Hall LM, Topinka AK, Sharpe SM, Leeson JY, Beckie HJ (2023) Increasing frequency of multiple herbicide-resistant kochia (*Bassia scoparia*) in Alberta. *Canadian Journal of Plant Science* 103, 233–237. <https://doi.org/10.1139/CJPS-2022-0224>
- Gleason HA, Cronquist A (1991) *Manual of Vascular Plants of Northeastern United States and Adjacent Canada*. 2nd ed. New York: New York Botanical Garden
- Goudet J, Jombart T (2022) hierfstat: Estimation and Tests of Hierarchical F-Statistics. R Package Version 0.5-11. <https://rdrr.io/cran/hierfstat/#:~:text=Estimates%20hierarchical%20F%2Dstatistics%20from,%2C%2052%3A950>. Accessed: Nov 15, 2023
- Graves S, Piepho H-P, Selzer L, Dorai-Raj S (2019) multcompView: Visualizations of Paired Comparisons. R Package Version 0.1-8. <https://cran.r-project.org/web/packages/multcompView/index.html>. Accessed Nov 1, 2022
- Grossmann K (2010) Auxin herbicides: current status of mechanism and mode of action. *Plant Manag Sci* 66:113–120
- Grossmann K, Hansen H (2001) Ethylene-triggered abscisic acid: a principle in plant growth regulation? *Physiol Plant* 113:9–14
- Grossmann K, Schmülling T (1995) The effects of the herbicide quinclorac on shoot growth in tomato is alleviated by inhibitors of ethylene biosynthesis and by the presence of an antisense construct to the 1-aminocyclopropane-1-carboxylic acid (ACC) synthase gene in transgenic plants. *Plant Growth Regul* 16:183–188

- Gu Z, Gu L, Eils R, Schlesner M, Brors B (2014) circlize: implements and enhances circular visualization in R. *Bioinformatics* 30:2811–2812
- Guo X-M, Wang Z-F, Zhang Y, Wang R-J (2021) Chromosomal-level assembly of the *Leptodermis oblonga* (Rubiaceae) genome and its phylogenetic implications. *Genomics* 113:3072–3082
- Gurevich A, Saveliev V, Vyahhi N, Tesler G (2013) QUASt: quality assessment tool for genome assemblies. *Bioinformatics* 29:1072–1075
- Hahne F, Ivanek R (2016) Visualizing genomics data using gviz and bioconductor. Pages 335–351 in Mathe E, Davis S, eds. *Statistical Genomics: Methods and Protocols*. New York: Springer
- Hall LM, Stromme KM, Horsman GP, Devine MD (1998) Resistance to acetolactate synthase inhibitors and quinclorac in a biotype of false cleavers (*Galium spurium*). *Weed Sci* 46:390–396
- Hall LM, Beckie HJ, Low R, Shirriff SW, Blackshaw RE, Kimmel N, Neeser C. (2014) Survey of glyphosate-resistant kochia (*Kochia scoparia* L. Schrad.) in Alberta. *Canadian Journal of Plant Science* 94, 127–130. <https://doi.org/10.4141/CJPS2013-204>
- Hansen H, Grossmann K (2000) Auxin-induced ethylene triggers abscisic acid biosynthesis and growth inhibition. *Plant Physiol* 124:1437–1448
- Harrell FE (2022) Hmisc: Harrell Miscellaneous. CRAN Version 4.7-2. <https://cran.r-project.org/web/packages/Hmisc/index.html>. Accessed: Nov 1, 2022
- Hashim S, Jan A, Sunohara Y, Hachinohe M, Ohdan H, Matsumoto H (2012) Mutation of alpha-tubulin genes in trifluralin-resistant water foxtail (*Alopecurus aequalis*). *Pest Manag Sci* 68:422–429
- Heap I (2023) The International Herbicide-Resistant Weed Database. weedscience.org/Home.aspx. Accessed: January 8, 2023
- Hervé M (2022) RVAideMemoire: Testing and Plotting Procedures for Biostatistics. R Package Version 0.9-81-2. <https://cran.r-project.org/web/packages/RVAideMemoire/index.html>. Accessed: Nov 1, 2022
- Hijmans RJ (2022) geosphere: Spherical Trigonometry. R Package Version 1.5-18. <https://cran.r-project.org/web/packages/geosphere/>. Accessed: Nov 1, 2022
- Hoff KJ, Lomsadze A, Borodovsky M, Stanke M (2019) Whole-genome annotation with BRAKER. *Methods Mol Biol* 1962:65–95
- Holm LG, Pancho JV, Herberger JP, Plucknett DL (1991) *A Geographical Atlas of World Weeds*. Malabar, FL: Krieger. 731 p
- Hu K, Xu K, Wen J, Yi B, Shen J, Ma C, Fu T, Ouyang Y, Tu J (2019) Helitron distribution in Brassicaceae and whole genome Helitron density as a character for distinguishing plant species. *BMC Bioinformatics* 20:354
- Jombart T (2008) adegenet: an R package for the multivariate analysis of genetic markers. *Bioinformatics* 24:1403–1405
- Kamvar Z, Tabima J, Grünwald N (2014) Poppr: an R package for genetic analysis of populations with clonal partially clonal and/or sexual reproduction. *PeerJ* 2:e281
- Kepinski S, Leyser O (2005) The *Arabidopsis* F-box protein TIR1 is an auxin receptor. *Nature* 435:446–451
- Kim D, Paggi JM, Park C, Bennett C, Salzberg SL (2019) Graph-based genome alignment and genotyping with HISAT2 and HISAT-genotype. *Nat Biotechnol* 37:907–915
- Knaus BJ, Grünwald NJ (2016) vcfR: a package to manipulate and visualize (VCF) data in R. *bioRxiv* 10.1101/041277
- Koren S, Walenz BP, Berlin K, Miller JR, Bergman NH, Phillippy AM (2017) Canu: scalable and accurate long-read assembly via adaptive k-mer weighting and repeat separation. *Genome Res* 27:722–736
- Kraft M, Kuglitsch R, Kwiatkowski J, Frank M, Grossmann K (2007) Indole-3-acetic acid and auxin herbicides up-regulate 9-cis-epoxycarotenoid dioxygenase gene expression and abscisic acid accumulation in cleavers (*Galium aparine*): interaction with ethylene. *J Exp Bot* 58:1497–1503
- Kumar S, Suleski M, Craig JE, Kasprócz AE, Sanderford M, Li M, Stecher G, Hedges SB (2022) TimeTree 5: an expanded resource for species divergence times. *Mol Biol Evol* 39:msac174
- Laetsch DR, Blaxter ML (2017) BlobTools: interrogation of genome assemblies. *F1000Research* 6:1287
- Lawrence M, Huber W, Pagès H, Aboyoun P, Carlson M, Gentleman R, Morgan M, Carey V (2013) Software for computing and annotating genomic ranges. *PLoS Comput Biol* 9:e1003118
- Leeson JY, Thomas AG, Hall LM, Brenzil CA, Andrews T, Brown KR, Van Acker RC (2005) *Prairie Weed Surveys of Cereal, Oilseed, and Pulse Crops from the 1970s to the 2000s*. Saskatoon, Canada: Agriculture and Agri-Food Canada. 395 p
- Lemon J (2006) plotrix: a package in the red light district of R. *R News* 6:8–12
- Li H, Durbin R (2009) Fast and accurate short read alignment with Burrows-Wheeler transform. *Bioinformatics* 25:1754–1760
- Li H, Handsaker B, Wysoker A, Fennell T, Ruan J, Homer N, Marth G, Abecasis G, Durbin R, Genome Project Data Processing S (2009) The sequence alignment/map format and SAMtools. *Bioinformatics* 25:2078–2079
- Li S-B, Xie Z-Z, Hu C-G, Zhang J-Z (2016) A review of auxin response factors (ARFs) in plants. *Front Plant Sci* 7:47
- Lomsadze A, Burns PD, Borodovsky M (2014) Integration of mapped RNA-seq reads into automatic training of eukaryotic gene-finding algorithms. *Nucleic Acids Res* 42:e119
- Looman J, Best KF (1979) *Budd's Flora of the Canadian Prairie Provinces*. Canada: Agriculture Canada. Hull, Quebec, Canada. 872 p
- Lovell JT (2023) GENESPACE: Synteny- and Orthology-constrained Comparative Genomics. R Package Version 1.0.13. <https://github.com/jtlovell/GENESPACE>. Accessed: Nov 15, 2023
- Lovell JT, Sreedasyam A, Schranz ME, Wilson M, Carlson J, Harkess A, Emms D, Goodstein DM, Schmutz J (2022) GENESPACE tracks regions of interest and gene copy number variation across multiple genomes. *eLife* 11:e78526
- Lu H, Yu Q, Han H, Owen MJ, Powles SB (2020) Evolution of resistance to HPPD-inhibiting herbicides in a wild radish population via enhanced herbicide metabolism. *Pest Manag Sci* 76:1929–1937
- Ludwig SR, Oppenheim DG, Silflow CD, Snustad DP (1987) Characterization of the a-tubulin gene family of *Arabidopsis thaliana*. *Proc Natl Acad Sci USA* 84:5833–5837
- Luo J, Zhou JJ, Zhang JZ (2018) Aux/IAA gene family in plants: molecular structure, regulation, and function. *Int J Mol Sci* 19:259
- Luu K, Bazin E, Blum MGB (2017) pcadapt: an R package to perform genome scans for selection based on principal component analysis. *Mol Ecol Res* 17:67–77
- Lysak MA (2022) Celebrating Mendel, McClintock, and Darlington: on end-to-end chromosome fusions and nested chromosome fusions. *Plant Cell* 34:2475–2491
- Malik N, Vanden Born WH (1988) The biology of Canadian weeds 86. *Galium aparine* L. and *Galium spurium* L. *Can J Plant Sci* 68:481–499
- Marçais G, Delcher AL, Phillippy AM, Coston R, Salzberg SL, Zimin A (2018) MUMmer4: a fast and versatile genome alignment system. *PLoS Comput Biol* 14:e1005944
- Martin SL, Benedict L, Wei W, Sauder CA, Beckie HJ, Hall LM (2020) High gene flow maintains genetic diversity following selection for high EPSPS copy number in the weed kochia (Amaranthaceae). *Sci Rep* 10:18864
- Martin SL, Smith TW, James T, Shalabi F, Kron P, Sauder CA (2017) An update to the Canadian range, abundance, and ploidy of *Camelina* spp. (Brassicaceae) east of the Rocky Mountains. *Botany* 95:405–417
- Mijangos JL, Gruber B, Berry O, Pacioni C, Georges A (2022) *dartR* v2: an accessible genetic analysis platform for conservation ecology and agriculture. *Methods Ecol Evol* 13:2150–2158
- Moore RJ (1975) The *Galium aparine* complex in Canada. *Can J Bot* 53:877–893
- Morgan M, Pagès H, Obenchain V, Hayden N (2021) Rsamtools: Binary Alignment (BAM), FASTA, Variant Call (BCF), and Tabix File Import. R Package Version 2.10.0. bioconductor.org/packages/Rsamtools. Accessed: Nov 1, 2022
- Nakka S, Godar AS, Wani PS, Thompson CR, Peterson DE, Roelofs J, Jugulam M (2017) Physiological and molecular characterization of hydroxyphenylpyruvate dioxygenase (HPPD)-inhibitor resistance in *Amaranthus palmeri*. *Front Plant Sci* 8:555
- Newcombe RG (1998) Two-sided confidence intervals for the single proportion: comparison of seven methods. *Stat Med* 17:857–872
- Oksanen J, Simpson GL, Blanchet FG, Kindt R, Legendre P, Minchin PR, O'Hara RB, Solymos P, Stevens MHH, Szoecs E, Wagner H, Barbour M, Bedward M, Bolker B, Borcard D, et al. (2022) *vegan*: Community Ecology Package. R Package Version 2.6-4
- O'Leary SJ, Puritz JB, Willis SC, Hollenbeck CM, Portnoy DS (2018) These aren't the loci you're looking for: principles of effective SNP filtering for molecular ecologists. *Mol Ecol* 27:3193–3206

- OpenAI (2024) ChatGPT (GPT-4). www.openai.com. Accessed Jul 28, 2024
- Ou S, Chen J, Jiang N (2018) Assessing genome assembly quality using the LTR Assembly Index (LAI). *Nucleic Acids Res* 46:e126
- Ou S, Jiang N (2018) LTR_retriever: a highly accurate and sensitive program for identification of long terminal repeat retrotransposons. *Plant Physiol* 176:1410–1422
- Ou S, Su W, Liao Y, Chougule K, Agda JRA, Hellings AJ, Lugo CSB, Elliott TA, Ware D, Peterson T, Jiang N, Hirsch CN, Hufford MB (2019) Benchmarking transposable element annotation methods for creation of a streamlined comprehensive pipeline. *Genome Biol* 20:275
- Pagès H, Aboyoun P, Gentleman R, DebRoy S (2021) Biostrings: Efficient Manipulation of Biological Strings. R Package Version 2.62.0. <https://rdrr.io/bioc/Biostrings/>. Accessed: Nov 1, 2022
- Paradis E (2010) pegas: an R package for population genetics with an integrated-modular approach. *Bioinformatics* 26:419–420
- Paradis E, Schliep K (2019) ape 5.0: an environment for modern phylogenetics and evolutionary analyses in R. *Bioinformatics* 35:526–528
- Pazmiño DM, Rodríguez-Serrano M, Romero-Puertas MC, Archilla-Ruiz A, Del Río LA, Sandalio LM (2011) Differential response of young and adult leaves to herbicide 2,4-dichlorophenoxyacetic acid in pea plants: role of reactive oxygen species. *Plant Cell Environ* 34:1874–1889
- Pebesma E (2018) Simple features for R: standardized support for spatial vector data. *R J* 10:439–446
- Pebesma E, Mailund T, Heibert J (2016) Measurement units in R. *R J* 8:486–494
- Peterson BK, Weber JN, Kay EH, Fisher HS, Hoekstra HE (2012) Double digest RADseq: an inexpensive method for de novo SNP discovery and genotyping in model and non-model species. *PLoS ONE* 7:e37135
- Pividori M (2024) Chatbots in science: what can ChatGPT do for you? *Nature*, August 14, 2024, <https://doi.org/10.1038/d41586-024-02630-z>
- Privé F, Luu K, Vilhjalmsón BJ, Blum MGB (2020) Performing highly efficient genome scans for local adaptation with R package pcadapt. *Mol Biol Evol* 37:2153–2154
- Quint M, Gray WM (2006) Auxin signaling. *Curr Opin Plant Biol* 9:448–453
- Rangani G, Salas-Perez RA, Aponte RA, Knapp M, Craig IR, Mietzner T, Langaro AC, Noguera MM, Porri A, Roma-Burgos N (2019) A novel single-site mutation in the catalytic domain of protoporphyrinogen oxidase IX (PPO) confers resistance to PPO-inhibiting herbicides. *Front Plant Sci* 10:568
- Revell LJ (2012) phytools: an R package for phylogenetic comparative biology (and other things). *Methods Ecol Evol* 3:217–223
- Revelle W (2023) psych: Procedures for Psychological Psychometric and Personality Research. R Package Version 2.3.6. <https://cran.r-project.org/web/packages/psych/index.html>. Accessed: Nov 15, 2023
- Savary P, Foltête J-C, Moal H, Vuidel G, Garnier S (2020) graph4lg: a package for constructing and analyzing graphs for landscape genetics in R. *Methods Ecol Evol* 1:1–9
- Scalabrín S, Toniutti L, Di Gaspero G, Scaglione D, Magris G, Vidotto M, Pinoso S, Cattonaro F, Magni F, Jurman I, Cerutti M, Suggi Liverani F, Navarini L, Del Terra L, Pellegrino G, et al. (2020) A single polyploidization event at the origin of the tetraploid genome of *Coffea arabica* is responsible for the extremely low genetic variation in wild and cultivated germplasm. *Sci Rep* 10:4642
- Schliep K, Jombart T, Kamvar ZN, Archer E, Harris R (2020) apex: Phylogenetic Methods for Multiple Gene Data. R Package Version 1.0.4. <https://cran.r-project.org/web/packages/apex/>. Accessed: Nov 1, 2022
- Schliep KP (2011) phangorn: phylogenetic analysis in R. *Bioinformatics* 27:592–593
- Shi J, Liang C (2019) Generic repeat finder: a high-sensitivity tool for genome-wide de novo repeat detection. *Plant Physiol* 180:1803–1815
- Simao FA, Waterhouse RM, Ioannidis P, Kriventseva EV, Zdobnov EM (2015) BUSCO: assessing genome assembly and annotation completeness with single-copy orthologs. *Bioinformatics* 31:3210–3212
- Smit A, Hubley R (2008–2015) RepeatModeler Open-1.0. www.repeatmasker.org. Accessed: Nov 1, 2022
- Smit A, Hubley R, Green P (2010–2013) RepeatMasker Open-4.0. www.repeatmasker.org. Accessed: Nov 1, 2022
- Smith T, Kron P, Martin S (2018) flowPloidy: an R package for genome size and ploidy assessment of flow cytometry data. *Appl Plant Sci* 6:e01164
- South A (2017) rnatuarearth: World Map Data from Natural Earth. R Package Version 0.1.0. <https://cran.r-project.org/web/packages/rnatuarearth/vignettes/rnatuarearth.html>. Accessed: Nov 1, 2022
- Soza VL, Olmstead RG (2010) Molecular systematics of tribe Rubieae (Rubiaceae): evolution of major clades, development of leaf-like whorls, and biogeography. *Taxon* 59:755–771
- Stanke M, Diekhans M, Baertsch R, Haussler D (2008) Using native and syntetically mapped cDNA alignments to improve de novo gene finding. *Bioinformatics* 24:637–644
- Stevens PF (2017) Angiosperm phylogeny website v14. www.mobot.org/mobot/research/apweb/welcom.html. Accessed: February 6, 2024
- Storey JD, Bass AJ, Dabney A, Robinson D (2022) qvalue: Q-Value Estimation for False Discovery Rate Control. R Package Version 2.28.0. <https://github.com/StoreyLab/qvalue>. Accessed: Nov 15, 2023
- Su W, Gu X, Peterson T (2019) TIR-Learner: a new ensemble method for TIR transposable element annotation provides evidence for abundant new transposable elements in the maize genome. *Mol Plant* 12:447–460
- Sun J, Wang J-x, Zhang H-j, Liu J-l, Bian S-n (2011) Study on mutations in ALS for resistance to tribenuron-methyl in *Galium aparine* L. *Agric Sci China* 10:86–91
- Sun P, Jiao B, Yang Y, Shan L, Li T, Li X, Xi Z, Wang X, Liu J (2022) WGDI: a user-friendly toolkit for evolutionary analyses of whole genome duplications and ancestral karyotypes. *Mol Plant* 15:1841–1851
- Tadeo K, Ronald K, Vereriano T, Robooni T (2024) Genetic diversity and structure of Ugandan tea (*Camellia sinensis* (L.) O. Kuntze) germplasm and its implication in breeding. *Genet Resour Crop Evol* 71:481–496
- Tan X, Calderon-Villalobos LIA, Sharon M, Zheng C, Robinson CV, Estelle M, Zheng N (2007) Mechanism of auxin perception by the TIR1 ubiquitin ligase. *Nature* 446:640–645
- R Core Team (2021) R: A Language and Environment for Statistical Computing. Version 4.1.1. Vienna, Austria: R Foundation for Statistical Computing. www.R-project.org
- Thioulouse J, Dray S, Dufour A-B, Siberchicot A, Jombart T, Pavoine S (2018) Multivariate Analysis of Ecological Data with ade4. New York: Springer. 329 p
- Todd OE, Figueiredo MRA, Morran S, Soni N, Preston C, Kubes MF, Napier R, Gaines TA (2020) Synthetic auxin herbicides: finding the lock and key to weed resistance. *Plant Sci* 300:110631
- Tranel PJ, Wright TR, Heap IM (2023) Mutations in Herbicide-Resistant Weeds to Inhibition of Acetolactate Synthase. www.weedscience.com. Accessed: August 9, 2023
- Turner NJ, Szczawinski AF (1978) Wild Coffee and Tea Substitutes of Canada. Ottawa: National Museum of Natural Sciences. 111 p
- Urbanek S (2022) png: Read and Write PNG Images. R Package Version 0.1-8. <https://cran.r-project.org/web/packages/png/index.html>. Accessed: Nov 15, 2023
- Van Eerd LL (2004) Characterization and Inheritance of Quinclorac Resistance in a False Cleavers (*Galium spurium* L.) Biotype. Doctoral dissertation. Guelph, Canada: University of Guelph. 199 p
- Van Eerd LL, McLean MD, Stephenson GR, Hall JC (2004) Resistance to quinclorac and ALS-inhibitor herbicides in *Galium spurium* is conferred by two distinct genes. *Weed Res* 44:355–365
- Van Eerd LL, Stephenson GR, Kwiatkowski J, Grossmann K, Hall JC (2005) Physiological and biochemical characterization of quinclorac resistance in a false cleavers (*Galium spurium* L.) biotype. *Pest Manag Sci* 53:1144–1151
- Venables WN, Ripley BD (2002) Modern Applied Statistics with S. 4th ed. New York: Springer. 498 p
- Voss EG, Reznicek AA (2012) Field Manual of Michigan Flora. Ann Arbor: University of Michigan Press. 1008 p
- Walker BJ, Abeel T, Shea T, Priest M, Abouelliel A, Sakthikumar S, Cuomo CA, Zeng Q, Wortman J, Young SK, Earl AM (2014) Pilon: an integrated tool for comprehensive microbial variant detection and genome assembly improvement. *PLoS ONE* 9:e112963
- Walsh TA, Neal R, Merlo AO, Honma M, Hicks GR, Wolff K, Matsumura W, Davies JP (2006) Mutations in an auxin receptor homolog AFB5 and in SGT1b confer resistance to synthetic picolinate auxins and not to 2,4-dichlorophenoxyacetic acid or indole-3-acetic acid in *Arabidopsis*. *Plant Physiol* 142:542–552

- Wang Y, Tang H, Debarry JD, Tan X, Li J, Wang X, Lee TH, Jin H, Marler B, Guo H, Kissinger JC, Paterson AH (2012) MCSanX: a toolkit for detection and evolutionary analysis of gene synteny and collinearity. *Nucleic Acids Res* 40:e49
- Wickham H (2016) ggplot2: Elegant Graphics for Data Analysis. Use R! New York: Springer. Second Edition. <https://doi.org/10.1007/978-1-4939-9723-8>. 260 p
- Wickham H (2022) stringr: Simple Consistent Wrappers for Common String Operations. R Package Version 1.5.0
- Wickham H, Averick M, Bryan J, Chang W, McGowan LDA, François R, Grolemund G, Hayes A, Henry L, Hester J, Kuhn M, Pedersen TL, Miller E, Bache SM, Müller K, et al. (2019) Welcome to the tidyverse. *J Open Source Softw* 4:1696
- Wickham H, François R, Müller HL (2022) dplyr: A Grammar of Data Manipulation. R Package Version 1.0.10. <https://cran.r-project.org/web/packages/dplyr/index.html>. Accessed: Nov 15, 2023
- Workman R, Renee F, Kilburn D, Hao S, Liu K, Timp W (2018) Recalcitrant plant species for third generation sequencing. *Protocol Exchange*. <https://doi.org/10.17504/protocols.io.4vbgw2n>. Accessed: July 05 2019
- Xiong W, He L, Lai J, Dooner HK, Du C (2014) HelitronScanner uncovers a large overlooked cache of Helitron transposons in many plant genomes. *Proc Natl Acad Sci USA* 111:10263–10268
- Xu Z, Wang H (2007) LTR_FINDER: an efficient tool for the prediction of full-length LTR retrotransposons. *Nucleic Acids Res* 35(Suppl 2):W265–W268
- Yamamoto E, Zeng L, Baird WV (1998) Alpha-tubulin missense mutations correlate with antimicrotubule drug resistance in *Eleusine indica*. *Plant Cell* 10:297–308
- Yang LE, Meng Y, Peng DL, Nie ZL, Sun H (2018) Molecular phylogeny of *Galium* L. of the tribe Rubieae (Rubiaceae)—emphasis on Chinese species and recognition of a new genus *Pseudogalium*. *Mol Phylogenet Evol* 126:221–232
- Zážímalová E, Murphy AS, Yang H, Hoyerová K, Hosek P (2010) Auxin transporters—why so many? *Cold Spring Harb Perspect Biol* 2:a001552
- Zážímalová E, Petrášek J, Benková E, Mueller-Roerber B, Balazadeh S (2014) Auxin and Its Role in Plant Development. Vienna: Springer. <https://doi.org/10.1007/978-3-7091-1526-8>. 444 p
- Zeileis A, Fisher J, Hornik K, Ihaka R, McWhite C, Murrell P, Stauffer R, Wilke C (2020) colorspace: a toolbox for manipulating and assessing colors and palettes. *J Stat Softw* 96:1–49
- Zhang R-G, Wang Z-X, Ou S, Li G-Y (2019) TESorter: lineage-level classification of transposable elements using conserved protein domains. *bioRxiv* 10.1101/800177
- Zheng H-g, Hall JC (2001) Understanding auxinic herbicide resistance in wild mustard: physiological, biochemical, and molecular genetic approaches. *Weed Sci* 49:276–281